```
Intectin   MRT-HLLWLLPLILL-----GSSAQALK C HE C SG---IED C YKPKT C SSQSLY C  45
mLy-6A     MDTSHTTKSCLLILLVALLCAERAQGLE C YQ C YGVPFETS C PS-IT C PYPDGV C  53
mLy-6C     MDSTHATKSCLLILLVALLCAGRAQGLQ C YE C YGVPIETS C PA-VT C RASDGF C  53
ThB        MKTA------LLVLLVLAVATSPAWALR C HV C TNSAN--- C KNPQV C PSNTYF C  45
TSA-1      MSATSNMRVFLPVLLAALLGMEQVHSLM C FS C TDQKNNIN C LWPVS C QEKDHY C  54

Intectin   LTNWYTPP-GQQTTVTKT--- C AYT C P-DINHVTA-----NSKSS CC NTDL C NSA  87
mLy-6A     VTQEAAVIVDSQTRKVK-NNL C LPI C PPNIESMEILGTKVNVKTS CC QEDL C NVA 107
mLy-6C     IAQNIELIEDSQRRKLKTRQ- C LSF C PAGVP---IKDPNIRERTS CC SEDL C NAA 104
ThB        KTVTSVEPLNGNL-VRKE--- C ANS C TSDYSQQGHVSSGSEV-TQ CC QTDL C NER  93
TSA-1      ITLSAAAGFGNVNLGYTLNKG C SPI C PS--ENVNLNLGVASVNSY CC QSSF C NFS 107

Intectin   RNLEVS-WG----LL-ALG---LCYIYLSQ                                111
mLy-6A     VPNGGSTWTMAGVLLFSLSSVLLQTLL                                    134
mLy-6C     VPTAGSTWTMAGVLLFSLSSVILQTLL                                    131
ThB        LVSAAPGHA----LLS---SVTLGLATSLSLLTVMALCL                        127
TSA-1      AAGLGLRASIP--LL-GLG-LLLSLLALLQLSP                              136
```

FIG. 2. **Amino acid alignments between intectin and other mouse Ly-6 proteins.** The amino acid sequence of intectin is aligned with other known mouse Ly-6 proteins. The highly conserved 10 cysteines in mouse Ly-6 proteins are indicated by *bold boxed letters*.

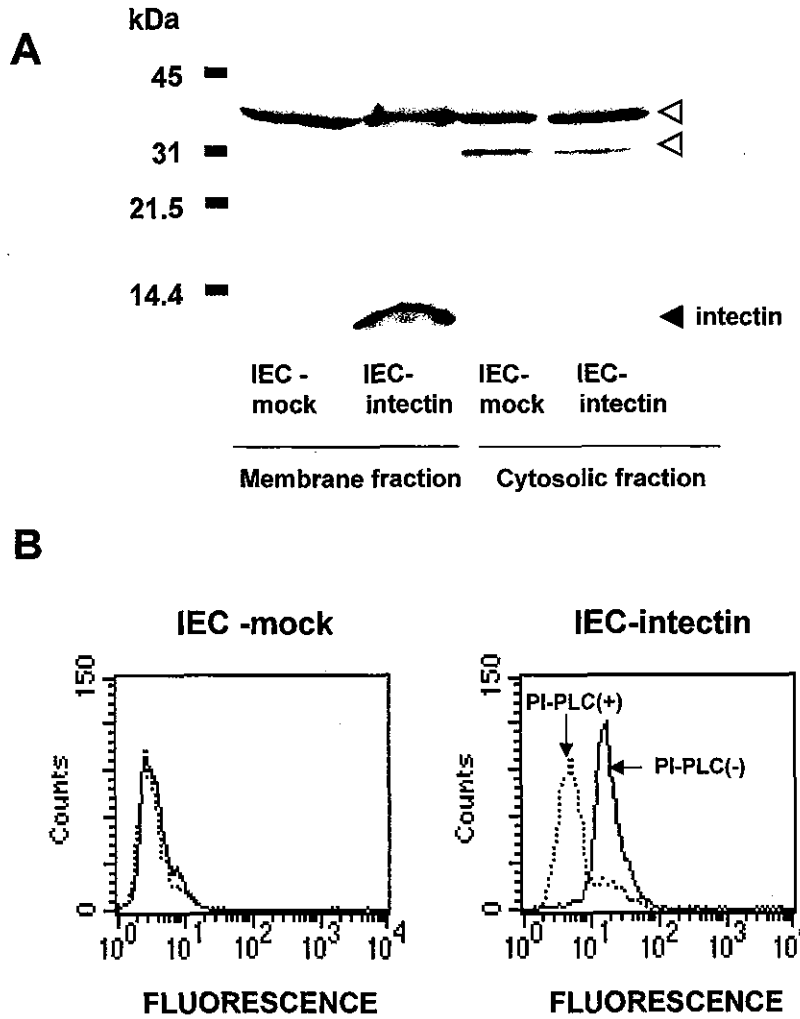

FIG. 3. **Expression of FLAG-tagged intectin on IEC-6 cell surface and sensitivity to PI-PLC.** *A*, location of intectin protein. The membrane fraction and cytosolic fraction of IEC-mock cells and IEC-intectin cells were subjected to Western blotting using anti-FLAG antibody. FLAG-tagged intectin protein is indicated by the *solid arrowhead*. Nonspecific bands are indicated by the *open arrowheads*. *B*, IEC-mock cells and IEC-intectin cells were treated with (*dotted line*) or without (*solid line*) PI-PLC for 1 h at 37 °C. Then, the cells were stained with FITC-conjugated anti-FLAG antibody and analyzed by flow cytometry.

cytes and in lymphoid organs, intectin mRNA expression was not detected in the bone marrow, WR19L (mouse T cell line), WEHI3 (mouse macrophage-like cell line), and BaF3 (mouse pro-B cell line) cells by quantitative RT-PCR (data not shown).

In situ hybridization was performed to determine the distribution of intectin mRNA in the intestine. Remarkably, a strong signal was detected only at the villus tips of the duodenum, jejunum, and ileum (Fig. 4, *B*, *E*, *H*, and *N*), and only a weak signal was detected in the colon (Fig. 4*K*), and a trace signal was found in the stomach and esophagus (data not shown). No signal was detected in all other tissues examined, including the brain, spleen, heart, lungs, eyes, lymph nodes, thyroid, skeletal muscles, thymus, liver, WAT, BAT, pituitary, adrenals, urinary bladder, gallbladder, and testes, by *in situ* hybridization (data not shown). Thus, intectin mRNA was exclusively expressed in the villus tips of the epithelial cells of the mouse small intestine. In this regard, Groos *et al.* (6) reported the exclusive presence of apoptotic cells at the villus tips in human and rat

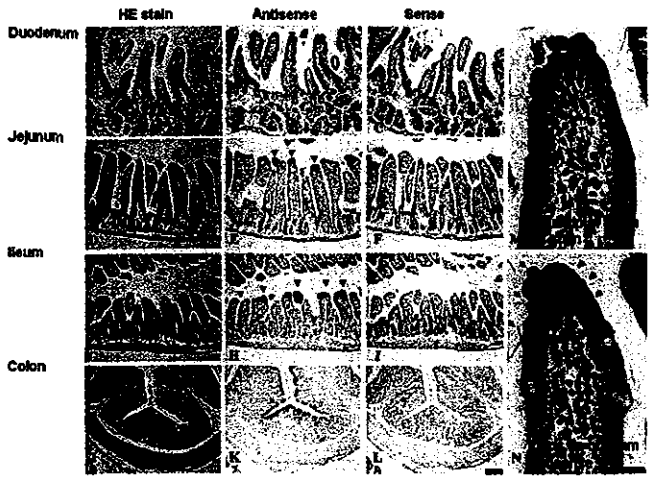

FIG. 4. **Intectin mRNA expression pattern in the mouse intestine.** *In situ* hybridization (ISH) revealed intectin antisense-specific signal (*black-purple*) at the villus tips of the duodenum (*A–C*), jejunum (*D–F*), and ileum (*G–I*) and in the covering epithelium of the colon (*J–L*) of C57BL/6 mouse (*arrowheads*). *A*, *D*, *G*, and *J*: hematoxylin-eosin stain; *B*, *E*, *H*, and *K*: ISH with intectin antisense probe; *C*, *F*, *I*, and *L*: intectin sense probe. Higher magnification of the villus tips of the ileum (*M*: H&E stain, *N*: ISH using intectin antisense probe and counterstained with hematoxylin (*blue*)) shows intectin antisense signal (*black-purple*) at the villus tips (*arrowheads*). *Scale bar* in *L* = 100 μm for *A–L* sections. *Scale bar* in *N* = 20 μm for *M* and *N* sections.

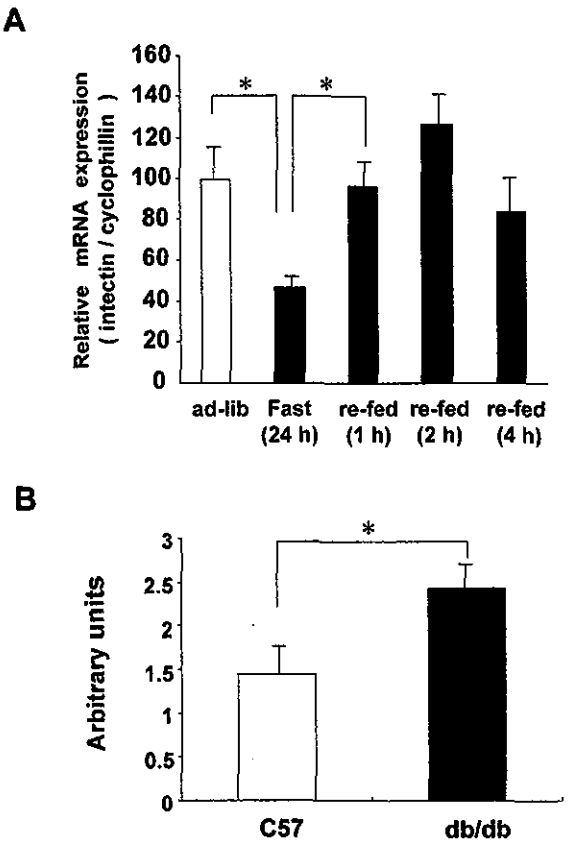

FIG. 5. **Nutritional modulation of intectin mRNA expression in mice.** *A*, modulation of intectin mRNA by fasting and refeeding. In these experiments, 6-week-old male C57BL/6J mice were fed *ad libitum*, fasted for 24 h, or fasted for 24 h and then re-fed 1, 2, and 4 h later (n = 3–4 mice for each group). Then, mice were sacrificed under anesthesia, and the small intestines were harvested immediately. Total RNA was extracted for real-time RT-PCR using intectin specific primers. Values are normalized to the level of cyclophilin mRNA and expressed as mean ± S.E. (n = 3–4). *, $p < 0.05$. *B*, comparison of intectin mRNA expression between C57BL/6J mice and genetically obese *db/db* mice. Intestines were excised from 6-week-old *db/db* mice and age-matched *ad libitum* fed C57BL6J mice. The mRNA was quantified by real-time RT-PCR as described above. Values are normalized to the level of cyclophilin mRNA and expressed as mean ± S.E. (n = 6). *, $p <$ 0.05, compared with *ad libitum* fed C57BL/6J mice.

small intestine epithelium. Thus, it is likely that the intectin-positive region is the same as that where apoptosis was identified by Groos *et al.* (6).

Intectin mRNA Expression Is Modulated by Nutritional Status—We next examined the nutritional regulation of intectin mRNA expression *in vivo* (Fig. 5*A*). Intectin mRNA expression in the small intestine was significantly decreased by 24-h fasting and restored to basal level by 1- to 2-h refeeding (Fig. 5*A*). These results indicate that intectin mRNA expression is modulated by nutritional stimuli. This conclusion was supported by our finding in *db/db* mice, whose daily food intake is 1.5- to 2-fold higher than that of age-matched C57BL/6J mice (data not shown); intectin mRNA expression in the small intestine of 6-week-old *db/db* mice was significantly higher than *ad libitum*-fed C57BL/6J mice (Fig. 5*B*).

Involvement of Intectin in the Rapid Turnover of Intestinal Mucosa—Based on its specific expression at the villus tips of the intestine and active nutritional regulation, we hypothesized that intectin could be involved in the rapid turnover of intestinal mucosa. To test our hypothesis, we first compared the viability of IEC-intectin cells and IEC-mock cells. Cell viability assay was performed after 12-h treatment with palmitate, a nutrient-derived inducer of apoptosis, or 24-h treatment with camptothecin and daunorubicin, chemical inducers of apoptosis. Palmitate treatment decreased cell viability of both IEC-intectin cells and IEC-mock cells, but the effect was significantly more pronounced in IEC-intectin cells than IEC-mock cells (Fig. 6*A*). For example, 6.3 μM palmitate reduced cell viability of IEC-intectin cells to 50%, whereas a similar change in cell viability of IEC-mock cells required 50 μM palmitate. On the other hand, there was no difference in cell viability between IEC-intectin cells and IEC-mock cells after treatment with camptothecin or daunorubicin (data not shown).

Intectin Induces Apoptosis of Intestinal Mucosal Cells via Caspase-3 Activation—Next, we compared the effects of palmitate on cell cycle in IEC-intectin cells and IEC-mock cells. For this purpose, the cells were incubated with palmitate and then stained with PI and sorted according to DNA content. As shown in Fig. 6*B*, cell cycle analysis by flow cytometry indicated that palmitate dose-dependently decreased the G_1 population, whereas it increased the sub-G_1 population and the cell death fraction, including apoptotic cells. These palmitate-induced changes in the cell cycle toward cell death were more pronounced in IEC-intectin cells compared with IEC-mock cells. For example, the majority of IEC-mock cells were in the G_1 or G_2 phase, while the majority of IEC-intectin cells were in the sub-G_1 phase when these cells were incubated in the presence of 50 or 100 μM palmitate (Fig. 6*B*).

To further examine the possible involvement of intectin in the rapid turnover of intestinal mucosa through cell death and especially through apoptosis, we measured caspase-3 activity in palmitate-treated IEC-intectin cells and IEC-mock cells (Fig. 6*C*). Because activation of caspase-3 is a common downstream effector of diverse apoptotic pathways (13), we measured cleavage of colorimetric substrate, specific to caspase-3. Low dose palmitate significantly increased caspase-3 activity in IEC-intectin cells compared with in IEC-mock cells. Taken together, the above results suggest that intectin expression causes activation of caspase-3, which in turn induces apoptotic death of IEC-6 cells.

Intectin Reduces Cell-to-Cell Adhesion—Previous studies suggested that some members of the Ly-6 family are involved

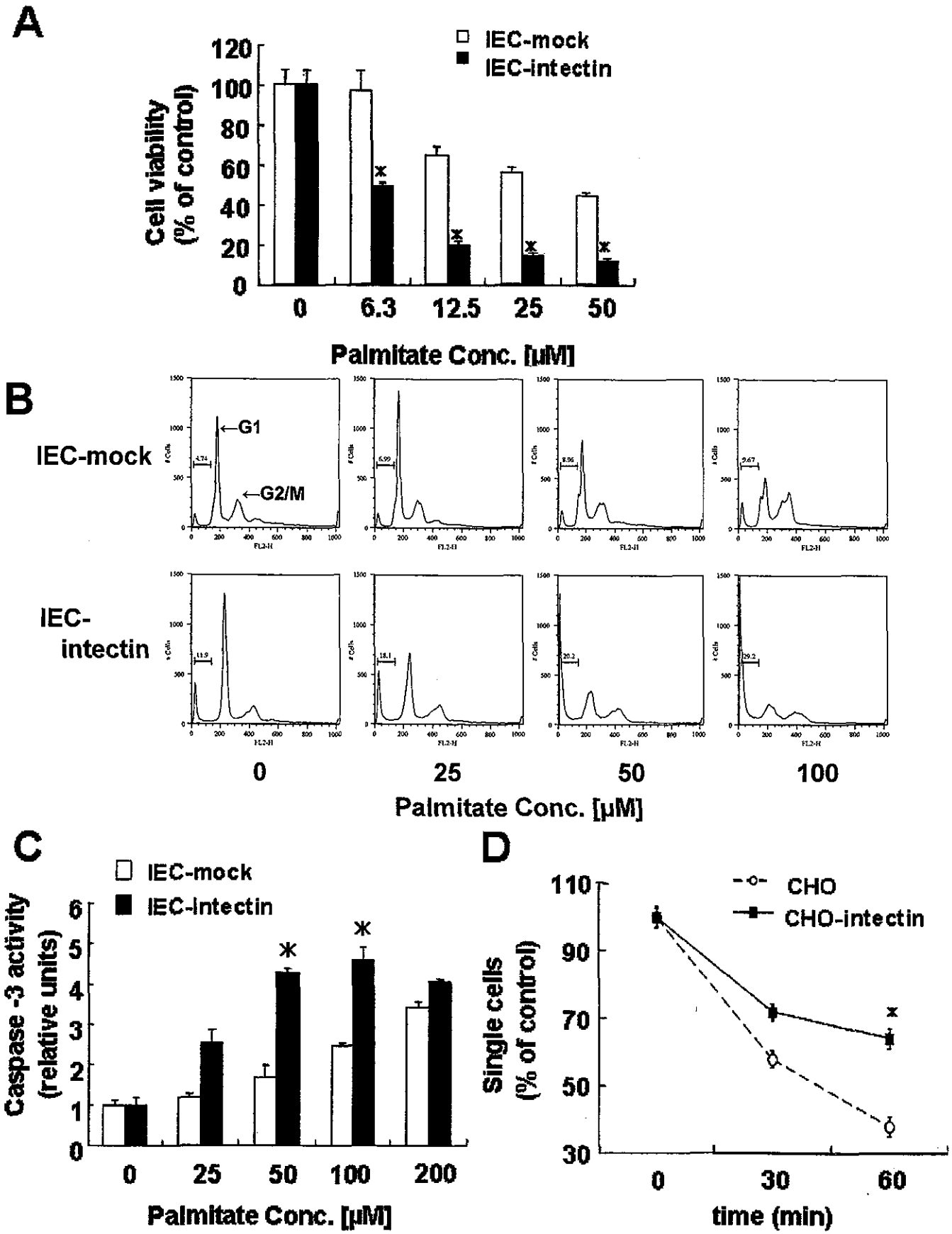

FIG. 6. **Effects of palmitate on apoptosis of IEC-6 cells.** *A*, effect of palmitate on viability of IEC-6 cells. IEC-intectin and IEC-mock cells were treated with palmitate. After 12-h treatment, the cells were treated with WST-8 and incubated for 1 h at 37 °C. The optical densities were measured at 450 and 650 nm. Values are expressed as mean ± S.E. ($n = 3$). *, $p < 0.05$. *B*, effect of palmitate on cell cycle. The cells were incubated with 0, 25, 50, or 100 μM palmitate for 12 h, and fixed with 70% cold ethanol. Then the samples were treated with 10 μg/ml RNase, stained with 10 μg/ml propidium iodide, and analyzed by flow cytometry. The sub-G_1 range is indicated by a *horizontal bar* above which the percentage of nuclei

in cell-cell adhesion (14, 15). Therefore, we conducted a cell aggregation assay using parental CHO cells (CHO) and CHO cells stably expressing intectin (CHO-intectin). Intectin expression significantly attenuated CHO cell aggregation (Fig. 6*D*), suggesting that intectin expression weakens the cell-cell adhesion probably to promote the exfoliation of intestinal epithelial cells.

DISCUSSION

The intestinal mucosa is continuously exposed to various toxic factors, including enteropathogenic microorganisms and food antigens. It also has to face potent digestive enzymes present in the lumen secreted from the liver and pancreas. In such harmful environments, the intestinal mucosa exhibits a rapid turnover, which serves to maintain the essential functions of the intestine and the integrity of the intestinal wall. The regulation of this rapid turnover of intestinal mucosa is complex and controlled by several factors. Apoptosis is one important factor that determines this process (16, 17). Therefore, identification of the regulatory factors of intestinal mucosal apoptosis should help us understand the mechanism of intestinal mucosal turnover.

In the present study, we identified intectin using an efficient SST technique. Although the precise physiological significance of intectin has yet to be determined, several important features were defined in the present study. 1) Intectin is a new member of GPI-anchored Ly-6 family; 2) intectin mRNA is exclusively expressed in the villus tips of the small intestine, which are known to undergo apoptosis; 3) intectin mRNA expression is influenced by nutritional changes; 4) intectin expression increases the sensitivity of intestinal epithelial cells to palmitate-induced apoptosis; and 5) intectin expression significantly attenuates cell aggregation. These findings suggest that intectin might modulate nutrition-dependent apoptosis, weaken cell-cell attachment, and promote the dying cells to exfoliate into the lumen at the final stage of intestinal mucosal turnover.

The intectin gene is located on murine chromosome 15, similar to murine *Ly-6* genes (18). The intectin protein is composed of 111 amino acid residues and has an Ly-6 domain, which is defined by a distinct disulfide-binding pattern between 10 cysteine residues. Furthermore, intectin protein has N-terminal and C-terminal signal sequences, and the result of PI-PLC treatment of intectin-expressing cells indicated that intectin was a GPI-anchored protein, a hallmark of Ly-6 family. These findings indicate that intectin is a novel member of the Ly-6 family. Previous studies suggested the involvement of Ly-6A/E in T-cell activation (19, 20) and development (21). Ly-6A/E and Ly-6C have been shown to regulate cell adhesion (14, 15), but the *in vivo* functions of Ly-6 family are unknown with the exception of CD59 and urokinase-type plasminogen activator receptor. CD59 functions as a membrane inhibitor of reactive lysis, and failure to express CD59 is related to the pathogenesis of paroxysmal nocturnal hemoglobinuria (PNH). In PNH, acquired somatic defect of the *PIG-A* gene results in a defect in GPI-anchored proteins expression, including CD59, on the cell surface, making blood cells more susceptible to host complement-mediated lysis (22, 23). These patients are more susceptible to leukemia (24) due to resistance to apoptosis caused by *PIG-A* gene mutations, suggesting that some of GPI-anchored proteins are important in modulating apoptosis (25). Considered together with the results of the present study, it is conceivable that intectin, a member of the GPI-anchored Ly-6 family proteins, is involved in the regulation of intestinal epithelial cell apoptosis.

Induction of apoptosis by palmitate has been reported in various cells, including pancreatic β-cells (26), cardiomyocytes (27), and hematopoietic cells (28). In the present study, we demonstrated that palmitate induced apoptosis of intestinal epithelial cells. Furthermore, recent studies reported nutritional modulation of intestinal mucosal apoptosis (29–31). Raab *et al.* (29) showed that high energy diet and purines in the diet induced intestinal mucosal apoptosis. In addition, Sukhotnik *et al.* (30) reported that exposure to low fat diet decreased intestinal epithelial cell apoptosis in a rat model of short bowel syndrome. These reports implicate nutrient-derived fat should induce apoptosis of intestinal epithelial cells. Groos *et al.* (31) also showed that apoptosis of intestinal epithelial cells at the villus tips was markedly reduced in subjects receiving total parenteral nutrition over 2 weeks compared with enterally nourished subjects, suggesting that food components seem to influence apoptosis of intestinal epithelial cells. The precise molecular mechanism that regulates apoptosis of intestinal mucosa in response to nutritional conditions has not yet been established. Since intectin mRNA expression was restored as fast as 1 h after refeeding following 24-h fasting, intectin expression is more likely regulated by food-related physical stimuli rather than by endocrine factors such as insulin. Palmitate is a major fatty acid in fat diet and is probably involved in fat diet-induced apoptosis of intestinal mucosa. Our finding that intectin accelerated palmitate-induced apoptosis of intestinal epithelial cells suggests that diet-induced expression of intectin might mediate this diet-induced apoptosis of intestinal mucosa.

Apoptotic cells are observed at the villus tips of intestinal mucosa. In certain inflammatory conditions, such as celiac disease, nematode infections, and graft-*versus*-host disease, the numbers of apoptotic nuclei were increased in villus epithelial cells (32–35). In addition, the involvement of dysregulation of the apoptotic process in intestinal epithelial cells in inflammatory bowel diseases and colon cancer has also been suggested (36, 37). These studies indicate that apoptosis plays some role in pathological conditions as well as in physiological turnover of villus epithelial cells. In this regard, whether intectin is involved in the pathology of inflammatory bowel diseases or colon cancer remains to be elucidated.

In conclusion, we described in this study the identification of intectin, a novel intestine-specific GPI-anchored protein. This protein enhanced palmitate-induced apoptosis of intestinal epithelial cells.

Acknowledgments—We thank the members of Shimomura's laboratory for the helpful discussions. We thank Drs. Yusuke Maeda and Taro Kinoshita (Osaka University) for kindly providing the pME-puro-FLAG-CD59 vector and for the helpful suggestions. We also thank Drs. Rikinari Hanayama and Shigekazu Nagata (Osaka University) for kindly providing the expression plasmid pEF-BOS and for the invaluable suggestions.

REFERENCES

1. Potten, C. S. (1992) *Cancer Metastasis Rev.* **11**, 179–195
2. Potten, C. S., and Allen, T. D. (1977) *J. Ultrastruct. Res.* **60**, 272–277
3. Williamson, R. C. (1978) *N. Engl. J. Med.* **298**, 1444–1450
4. Jones, B. A., and Gores, G. J. (1997) *Am. J. Physiol.* **273**, G1174–G1188
5. Potten, C. S. (1997) *Am. J. Physiol.* **273**, G253–G257

containing the sub-G_1 amount of DNA is indicated. *C*, IEC-intectin and IEC-mock cells were incubated with 0, 25, 50, 100, or 200 μM palmitate for 12 h. Caspase-3 activity was measured as described under "Experimental Procedures." Values are expressed as mean ± S.E. ($n = 4$). *, $p < 0.05$, compared with IEC-mock cells. *D*, cell aggregation assay. Parental CHO cells and CHO-intectin cells were subjected to aggregation assay as described under "Experimental Procedures." Cells remaining as single cells were counted at indicated periods of time. The number of cells present in aggregates was also counted. Values are expressed as mean ± S.E. ($n = 4$). *, $p < 0.05$, compared with parental CHO cells.

6. Groos, S., Reale, E., and Luciano, L. (2003) *Anat. Rec.* **272,** 503–513
7. Kojima, T., and Kitamura, T. (1999) *Nat. Biotechnol.* **17,** 487–490
8. Nishizawa, H., Shimomura, I., Kishida, K., Maeda, N., Kuriyama, H., Nagaretani, H., Matsuda, M., Kondo, H., Furuyama, N., Kihara, S., Nakamura, T., Tochino, Y., Funahashi, T., and Matsuzawa, Y. (2002) *Diabetes* **51,** 2734–2741
9. Uchida, E., Mizuguchi, H., Ishii-Watabe, A., and Hayakawa, T. (2002) *Biol. Pharmacol. Bull.* **25,** 891–897
10. Whittard, J. D., and Akiyama, S. K. (2001) *Exp. Cell Res.* **263,** 65–76
11. Kyte, J., and Doolittle, R. F. (1982) *J. Mol. Biol.* **157,** 105–132
12. Johnson, R., Lancki, D. W., and Fitch, F. W. (1993) *J. Immunol.* **151,** 2986–2999
13. Green, D. R. (2000) *Cell* **102,** 1–4
14. Bamezai, A., and Rock, K. L. (1995) *Proc. Natl. Acad. Sci. U. S. A.* **92,** 4294–4298
15. Hanninen, A., Jaakkola, I., Salmi, M., Simell, O., and Jalkanen, S. (1997) *Proc. Natl. Acad. Sci. U. S. A.* **94,** 6898–6903
16. Potten, C. S., Wilson, J. W., and Booth, C. (1997) *Stem Cells* **15,** 82–93
17. Hall, P. A., Coates, P. J., Ansari, B., and Hopwood, D. (1994) *J. Cell Sci.* **107,** 3569–3577
18. LeClair, K. P., Rabin, M., Nesbitt, M. N., Pravtcheva, D., Ruddle, F. H., Palfree, R. G., and Bothwell, A. (1987) *Proc. Natl. Acad. Sci. U. S. A.* **84,** 1638–1642
19. Flood, P. M., Dougherty, J. P., and Ron, Y. (1990) *J. Exp. Med.* **172,** 115–120
20. Lee, S. K., Su, B., Maher, S.E., and Bothwell, A. L. (1994) *EMBO J.* **13,** 2167–2176
21. Bamezai, A., Palliser, D., Berezovskaya, A., McGrew, J., Higgins, K., Lacy, E., and Rock, K. L. (1995) *J. Immunol.* **154,** 4233–4239
22. Kinoshita, T., Ohishi, K., and Takeda, J. (1997) *J. Biochem. (Tokyo)* **122,** 251–257
23. Rosse, W. F., and Ware, R. E. (1995) *Blood* **86,** 3277–3286
24. Horikawa, K., Nakamura, H., Kawaguchi, T., Iwamoto, N., Nagakura, S., Kagimoto, T., and Takatsuki, K. (1997) *Blood* **90,** 2716–2722
25. Brodsky, R. A., Vala, M. S., Barber, J. P., Medof, M. E., and Jones, R. J. (1997) *Proc. Natl. Acad. Sci. U. S. A.* **94,** 8756–8760
26. Shimabukuro, M., Zhou, Y. T., Levi, M., and Unger, R. H. (1998) *Proc. Natl. Acad. Sci. U. S. A.* **95,** 2498–2502
27. Sparagna, G. C., Hickson-Bick, D. L., Buja, L. M., and McMillin, J. B. (2001) *Antioxid. Redox. Signal.* **3,** 71–79
28. Paumen, M. B., Ishida, Y., Muramatsu, M., Yamamoto, M., and Honjo, T. (1997) *J. Biol. Chem.* **272,** 3324–3329
29. Raab, S., Leiser, R., Kemmer, H., and Claus, R. (1998) *Metabolism* **47,** 1105–1111
30. Sukhotnik, I., Shiloni, E., Krausz, M. M., Yakirevich, E., Sabo, E., Mogilner, J., Coran, A. G., and Harmon, C. M. (2003) *J. Pediatr. Surg.* **38,** 1182–1187
31. Groos, S., Reale, E., Hunefeld, G., and Luciano, L. (2003) *J. Surg. Res.* **109,** 74–85
32. Moss, S. F., Attia, L., Scholes, J. V., Walters, J. R., and Holt, P. R. (1996) *Gut* **39,** 811–817
33. Hyoh, Y., Nishida, M., Tegoshi, T., Yamada, M., Uchikawa, R., Matsuda, S., and Arizono, N. (1999) *Parasitology* **119,** 199–207
34. Hyoh, Y., Ishizaka, I., Horii, T., Fujiwara, A., Tegoshi, T., Yamada, M., and Arizono, N. (2002) *Gut* **50,** 71–77
35. Stuber, E., Buschenfeld, A., von Freier, A., Arendt, T., and Folsch, U. R. (1999) *Gut* **45,** 229–235
36. Ruemmele, F. M., Seidman, E. G., and Lentze, M. J. (2002) *J. Pediatr. Gastroenterol. Nutr.* **34,** 254–260
37. Shanmugathasan, M., and Jothy, S. (2000) *Pathol. Int.* **50,** 273–279

THE JOURNAL OF BIOLOGICAL CHEMISTRY
Vol. 279, No. 19, Issue of May 7, pp. 19391–19395, 2004
Printed in U.S.A.

Musclin, a Novel Skeletal Muscle-derived Secretory Factor*[S]

Received for publication, February 10, 2004, and in revised form, March 2, 2004
Published, JBC Papers in Press, March 24, 2004, DOI 10.1074/jbc.C400066200

Hitoshi Nishizawa‡§ §§, Morihiro Matsuda‡§ §§, Yukio Yamada‡§¶, Kenichiro Kawai‡, Emi Suzuki‡‖, Makoto Makishima‡, Toshio Kitamura, and Iichiro Shimomura‡‖‡‡**

*From the ‡Department of Medicine and Pathophysiology, Graduate School of Frontier Bioscience, Graduate School of Medicine, Osaka University, 2-2 Yamadaoka, Suita, Osaka 565-0871, the **Department of Hematopoietic Factors, Institute of Medical Science, University of Tokyo, Minato-ku, Tokyo 108-8639, ‖PREST, Japan Science and Technology Agency, 4-1-8 Honcho, Kawaguchi, Saitama 332-0012, and the §§21st Century COE Program, the Japan Society for the Promotion of Science, Tokyo 102-8471, Japan*

Skeletal muscle is involved in the homeostasis of glucose and lipid metabolism. We hypothesized that the skeletal muscle produces and secretes bioactive factor(s), similar to adipocytokines secreted by fat tissue. Here, we report the identification of a novel secretory factor, musclin, by signal sequence trap of mouse skeletal muscle cDNAs. Musclin cDNA encoded 130 amino acids, including NH_2-terminal 30-amino acid signal sequence. Musclin protein contained a region homologous to natriuretic peptide family, and KKKR, a putative serine protease cleavage site, similar to the natriuretic peptide family. Full-length musclin protein and KKKR-dependent cleaved form were secreted *in media* of musclin cDNA-transfected mammalian cell cultures. Musclin mRNA was expressed almost exclusively in the skeletal muscle of mice. Musclin mRNA levels in skeletal muscle were markedly low in fasted, increased upon re-feeding, and were low in streptozotocin-treated insulin-deficient mice. Musclin mRNA expression was induced at late stage in the differentiation of C2C12 myocytes. In myocytes, *insulin* increased, while epinephrine, isoproterenol, and forskolin reduced musclin mRNA, all of which are known to increase the cellular content of cyclic AMP, a counter-regulator to insulin. Pathologically, overexpression of musclin mRNA was noted in the muscles of obese insulin-resistant KKAy mice. Functionally, recombinant musclin significantly attenuated insulin-stimulated glucose uptake and glycogen synthesis in myocytes. In conclusion, we identified musclin, a novel skeletal muscle-derived secretory factor. Musclin expression level is tightly regulated by nutritional changes and its physiological role could be linked to glucose metabolism.

Adipose tissue has been shown to produce secretory factors conceptualized adipocytekines (1, 2).

Muscle-specific glucose transporter GLUT4[1] (3) and peroxisome proliferator-activated receptor-γ (4, 5) knock-out mice exhibited the alterations in insulin sensitivity in fat and liver. Muscle-specific insulin receptor knockout mice showed adipocyte hyperproliferation (6). These findings suggest that the skeletal muscle may release bioactive factors (*myokines*), like adipocytokines, to target fat, liver, and potentially skeletal muscle itself.

In the present study, we attempted to identify skeletal muscle-derived secretory factors using an efficient signal sequence trap (SST) method (7). Here, we report a novel skeletal muscle-derived secretory factor, musclin, whose mRNA was dynamically regulated by nutrition and hormonal factors.

EXPERIMENTAL PROCEDURES

Cloning of Mouse Musclin cDNA—Poly(A)$^+$ RNAs were extracted from gastrocnemius muscles of 10-week-old male C57BL/6J mice under *ad libitum*, 24-h fasting or 24-h refeeding after 24-h fasting condition and *ad libitum db/db* mice. Equal amounts of poly(A)$^+$ RNA from each group were pooled to synthesize cDNA. To selectively clone the genes that possess signal sequence at the NH_2-terminal end of cDNAs, SST-REX system (signal sequence trap by retrovirus-mediated expression screening system) was introduced as we reported previously (7). Interleukin-3-independent Ba/F3 cells were harvested, and the integrated cDNAs were isolated from the cells by genomic PCR and sequenced.

To identify full-length cDNA sequence of musclin, the original fragment obtained by SST-REX system was subjected to 5′- and 3′-RACE, using SMART™ RACE cDNA amplification kit (BD Biosciences). Rat and human full-length cDNA were cloned, using homology search for rat and human genome (GenBank™) with mouse musclin sequence, RACE, and reverse transcription-PCR.

Animals and Experimental Protocol—Male C57BL/6J mice (10 weeks old) were divided into three groups ($n = 5$, each): mice fed *ad libitum* with standard chow, mice fasted for 48 h, and mice refed 24 h after 48-h fasting.

Male C57BL/6J mice (10 weeks old) received one-shot intraperitoneal injection of streptozotocin (STZ, Sigma) (100 mg/kg body weight) every day for 3 days (total three times). The mice were sacrificed 4 days after the final injection.

Musclin mRNA expression in various tissues of mice was analyzed in 10–12-week-old male C57BL/6J mice. Musclin mRNA expression was also analyzed in muscles of 13-week-old female C57BL/6J and KKAy mice.

All experimental protocols were approved by the Ethics Review Committee for Animal Experimentation of Osaka University.

Northern Blot and Quantitative Reverse Transcription-PCR Analysis—RNA extraction and Northern blotting were conducted as described previously (8). First strand cDNA was synthesized using Ther-

* This work was supported in part by the Suzuken Memorial Foundation; The Nakajima Foundation; the Kanae Foundation for Life and Socio-Medical Science; the Takeda Medical Research Foundation; the Takeda Science Foundation; a grant-in-aid from the Japan Medical Association; The Naito Foundation; by a grant from the Ministry of Health, Labor and Welfare, Japan; and by grants from the Ministry of Education, Culture, Sports, Science and Technology, Japan. The costs of publication of this article were defrayed in part by the payment of page charges. This article must therefore be hereby marked "*advertisement*" in accordance with 18 U.S.C. Section 1734 solely to indicate this fact.

[S] The on-line version of this article (available at http://www.jbc.org) contains Supplemental Figs. 1 and 2.

The nucleotide sequence(s) reported in this paper has been submitted to the GenBank™/EBI Data Bank with accession number(s) AY573932, AY573933, and AY573934.

§ These authors contributed equally to this study.

¶ Present address: Takeda Chemical Industries, Ltd., Yodogawa-ku, Osaka 532-8686, Japan.

‡‡ To whom correspondence should be addressed: Dept. of Medicine and Pathophysiology, Graduate School of Frontier Bioscience, Graduate School of Medicine, Osaka University, 2-2 Yamadaoka H2, Suita, Osaka 565-0871, Japan. Tel.: 81-6-6879-3272; Fax: 81-6-6879-3279; E-mail: ichi@fbs.osaka-u.ac.jp.

[1] The abbreviations used are: GLUT, glucose transporter; 2-DG, 2-deoxy-D-glucose; ANP, atrial natriuretic peptide; BNP, brain natriuretic peptide; CNP, c-type natriuretic peptide; HEK, human embryonic kidney; IGF, insulin like growth factor; SST-REX, signal sequence trap by retrovirus-mediated expression screening; STZ, streptozotocin; RACE, rapid amplification of cDNA ends; RT, reverse transcription.

moScript RT-PCR System (Invitrogen). Quantitative RT-PCR was performed on LightCycler using the FastStart DNA Master SYBR Green I (Roche Diagnostics). The primers of mouse musclin for quantitative PCR are: 5′-TGTGGACTTAGCATCACAGG-3′ and 5′-AGCTGAGAGTCTGTCAAGG-3′.

Effects of Various Hormones on Musclin mRNA Expression in C2C12 Myocytes—Mouse myoblast cell line C2C12 cells were grown and induced for differentiation, as described previously (9). Cells were harvested at the indicated time. The effects of insulin, IGF-1, epinephrine, isoproterenol, forskolin, and vehicle on musclin mRNA expression were examined in differentiated C2C12 myocytes (day 7). After 24-h incubation with serum-free Dulbecco's modified Eagle's medium containing the test hormone, the cells were harvested for measurement of mRNA.

Stable Cell Lines Expressing FLAG-tagged Musclin—A retrovirus carrying full-length mouse musclin with FLAG epitope (DYKDDDDK) at the C terminus or green fluorescent protein was generated as described previously (7). The virus was added to C2C12 cells, and after puromycin selection, virus-infected stable C2C12 cells were differentiated to myocytes. Seven days after differentiation induction, the medium was collected, and cells were lysed with extraction buffer as described previously (8) and subjected to immunoprecipitation with anti-FLAG antibody (anti-FLAG M2-agarose gel, A2220, Sigma), followed by Western blotting using anti-FLAG M2 monoclonal antibody (A8592, Sigma).

Secretion of Wild-type and Mutant Musclin—The cDNA encoding mouse musclin protein fused to COOH-terminal FLAG epitope or mutant musclin protein fused to COOH-terminal FLAG (the ^{76}KKKR^{79} was changed to ^{76}A, using a QuikChange site-directed mutagenesis kit, Stratagene) was subcloned into pEF-BOS expression plasmid (pEF-BOS-WT musclin FLAG and pEF-BOS-Mut musclin FLAG, respectively) (10). HEK293 cells were transfected with pEF-BOS-WT musclin FLAG or pEF-BOS-Mut musclin FLAG. After 72 h, the culture medium was subjected to immunoprecipitation with anti-FLAG antibody, followed by Western blotting using anti-FLAG antibody.

Preparation of Recombinant Musclin Protein—Recombinant musclin protein was purified from culture medium of stable C2C12 myocytes expressing FLAG-tagged musclin using agarose beads column conjugating anti-FLAG antibody (anti-FLAG M2-agarose gel, A2220, Sigma).

Glucose Uptake and Glycogen Synthesis in C2C12 Skeletal Muscle Cells—Glucose uptake and glycogen synthesis were assayed using 2-deoxy-D-[1-^{3}H]glucose (2-DG) and D-[1-^{14}C]glucose, respectively. Differentiated C2C12 myocytes (day 5) were used. Cells were pretreated for 5 h with fetal calf serum-free Dulbecco's modified Eagle's medium (serum starvation) containing FLAG-tagged musclin (0.5 μg/ml) or FLAG peptide as control. For 2-DG uptake, the cells were incubated with or without insulin (100 nM) for 30 min, as described previously (9). For glycogen synthesis, the cells were incubated with or without insulin (100 nM) for 1 h, as described previously (11).

Statistical Analysis—Statistical analyses were performed with unpaired *t* tests, except for data shown in Fig. 3, *B* and *D–F*. Statistical analyses of the data shown in Fig. 3, *B* and *D–F*, were performed with analysis of variance (Fisher's projected least significant difference). A p value less than 0.05 denoted the presence of a statistically significant difference.

RESULTS

We previously developed an efficient SST method using retrovirus-mediated gene transfer (7). To identify skeletal muscle-derived nutritionally regulated secretory factor(s), we conducted this SST method using the pooled poly(A)$^+$ RNA from gastrocnemius muscles of mice under *ad libitum*, fasted and refed conditions, and obese diabetic *db/db* mice. We screened and sequenced 1812 clones. 18 clones were selected as unknown putative secreted proteins with a signal sequence and no putative transmembrane region. The mRNA of one clone was almost exclusively expressed in the skeletal muscle. The original fragment obtained from SST-REX screening was subjected to 5′- and 3′-RACE to obtain the non-coding region of musclin. The encoded protein was previously unidentified and was named musclin (Fig. 1*A*). Musclin consisted of 130 amino acids, including an amino-terminal 30-amino acid signal sequence, with a predicted molecular mass of 11 kDa. Rat and human coding regions of cDNAs were cloned using homology search for rat and human genome (GenBank™) with mouse musclin sequence, RACE, and RT-PCR (Fig. 1*B*). Amino acid sequence identity between mouse and human was 75.9% and that between mouse and rat was 90.2%. COOH terminus of the protein contained a region highly homologous to mouse natriuretic peptide including ANP, BNP, and CNP (12). A KKKR putative serine protease cleavage site also existed prior to this homologous region, similar to the NPs. These motifs suggested that musclin protein might also excise cleaved form at KKKR site, similar to natriuretic peptide.

To investigate whether musclin is a myosecretory protein, we constructed a mouse myoblast C2C12 cell line stably expressing a FLAG epitope-tagged musclin with a retrovirus. The cell lysate and medium of these cells were immunoprecipitated with anti-FLAG antibody and subjected to Western blotting with anti-FLAG antibody. Differentiated C2C12 myocytes synthesized the musclin protein as seen in cell lysate, and the synthesized protein was robustly secreted into the medium (Fig. 1*C*), indicating that musclin is a secretory protein. Three bands were detected in blots of musclin. Two bands positioned between 15 and 20 kDa. These sizes were different from the deduced size of 11 kDa, suggesting that musclin protein undergoes post-translational modification. The third band, whose abundance was extremely low in this cell system expressing FLAG-tagged musclin protein, positioned at about 12–13 kDa, suggesting that musclin protein was cleaved at the ^{76}KKKR^{79} site as described above. To test this, expression plasmid carrying wild-type or mutant musclin (^{76}KKKR$^{79}\rightarrow^{76}$A) fused to FLAG at the COOH terminus was transiently transfected in HEK293 cells, and the culture medium was subjected to immunoprecipitation and Western blotting with FLAG antibody (Fig. 1*D*). The mutated musclin did not produce the cleaved form, suggesting that some amount of wild-type musclin protein was cleaved at the ^{76}KKKR^{79} site.

When various tissues of C57BL/6J mice were subjected to Northern blotting, musclin mRNA was almost exclusively expressed in skeletal muscles (Fig. 2*A*), and the mRNA length was about 1.4 kb. By real-time RT-PCR analysis, musclin mRNA was also expressed in brown adipose tissue, spleen, testis, and bone to a much lesser extent than skeletal muscle (Fig. 2*B*). Rat musclin mRNA was also expressed almost exclusively in skeletal muscle (data not shown).

We examined regulation of musclin mRNA expression *in vivo* (Fig. 2, *C–E*). Musclin mRNA expression in gastrocnemius muscle was almost eliminated by 48-h fasting and reversed by 24-h refeeding (Fig. 2*C*). This nutritional regulation of musclin mRNA was much more dramatic than those of GLUT4 and lipoprotein lipase mRNAs (Supplemental Fig. 1). To determine the effect of insulin on musclin mRNA expression, mice were treated with STZ. Musclin mRNA expression was significantly decreased in the gastrocnemius muscles of STZ-treated insulin-deficient mice (Fig. 2*D*). With regard to pathophysiological significance, musclin mRNA expression was augmented in gastrocnemius muscle of obese KKAy mice, at both diabetic (13-week-old) (Fig. 2E) and non-diabetic (7-week-old) stages (data not shown). A similar increase of musclin mRNA was observed in the skeletal muscles of obese *db/db* mice (data not shown).

Next, we analyzed musclin mRNA expression in mouse myoblast cell line, C2C12. Musclin mRNA was not detected before induction (day 0) and markedly induced after differentiation of C2C12 myotubes, reaching a peak level at a later stage of differentiation (Fig. 3*A*), compared with mRNAs of other myogenic proteins, such as myogenin, GLUT4, PGC-1α, and UCP3 (Supplemental Fig. 2*A*). Recombinant musclin and retrovirus-mediated expression of musclin protein had no effect on proliferation and differentiation of C2C12 myoblasts, suggesting musclin had no significant effect on myogenesis (data not

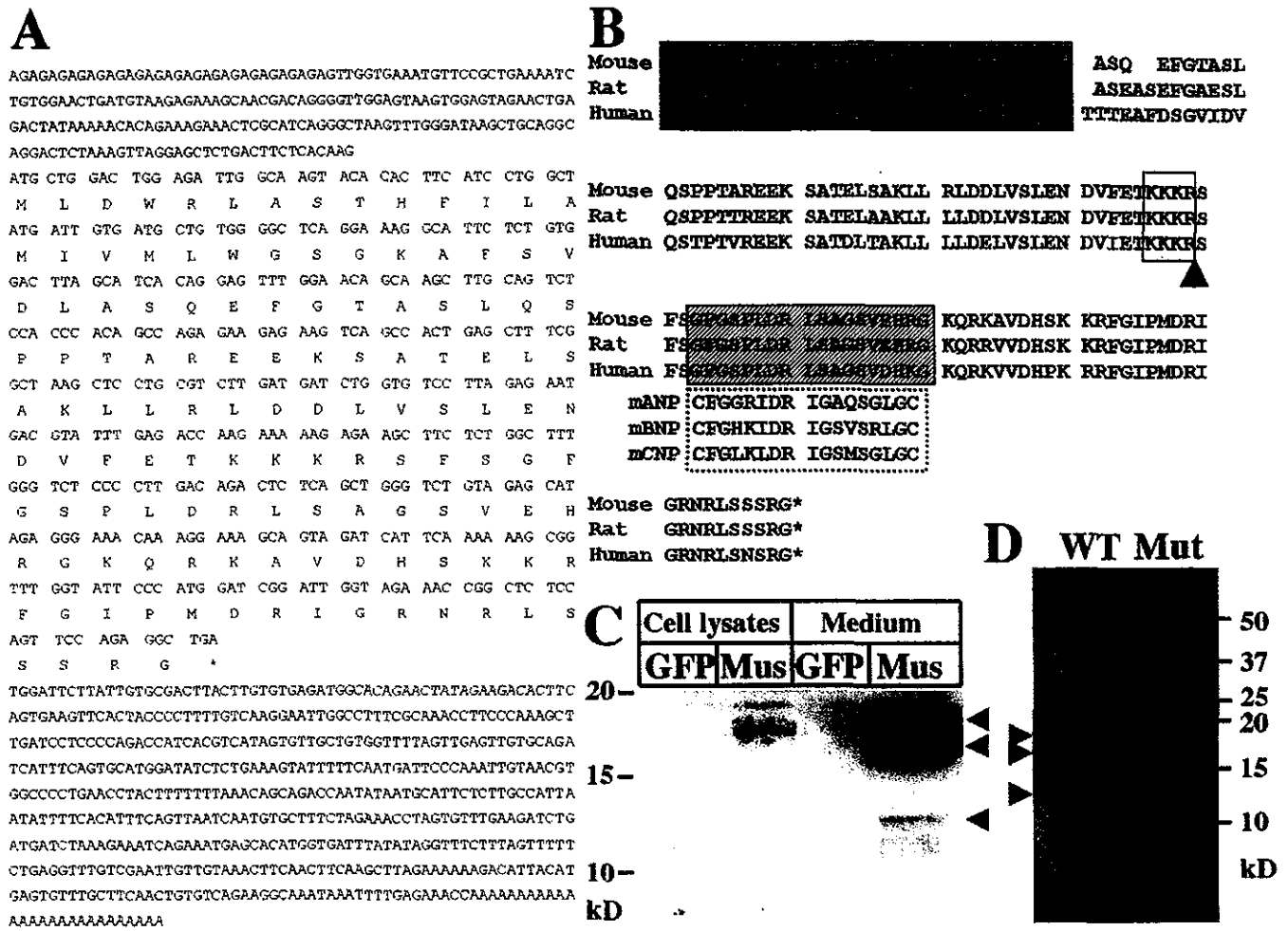

FIG. 1. **Nucleotide and deduced amino acid sequence of musclin.** *A*, nucleotide and deduced amino acid sequence of mouse musclin. *B*, alignments of musclin amino acid sequences for mouse, rat, and human. *Shaded box*, predicted signal sequence. *Open box*, the putative serine protease cleavage site, KKKR. *Hatched box*, the region homologous to mouse ANP, BNP, and CNP. *C*, secretion of musclin protein. The cell lysates and culture medium from C2C12 myocytes infected by retrovirus carrying FLAG-tagged mouse musclin or green fluorescent protein were immunoprecipitated and subjected to Western blot analysis, using anti-FLAG antibody. *Mus*, musclin. *D*, secretion of wild-type and mutant musclin from HEK293 cells. The culture medium from HEK293 cells transfected with pEF-BOS-WT musclin FLAG (*left lane*) or pEF-BOS-Mut musclin FLAG (^{76}KKKR^{79}→^{76}A) (*right lane*) was subjected to immunoprecipitation followed by Western blotting using anti-FLAG antibody.

shown). These results suggested that the physiological significance of musclin is related to some yet unknown function of fully differentiated myocytes.

We also examined the regulation of musclin mRNA in fully differentiated C2C12 myocytes (day 7). Insulin markedly and dose-dependently augmented musclin mRNA expression (Fig. 3*B*), but not that of myogenin, a myocyte differentiation marker gene (Supplemental Fig. 2*B*), suggesting that insulin-stimulated musclin mRNA expression in myocytes was not due to overdifferentiation of myocytes but rather to direct induction of musclin mRNA. IGF-1 also induced musclin mRNA expression (Fig. 3*B*). On the other hand, epinephrine and β-adrenergic receptor agonist, isoproterenol, counter-regulators to insulin in glucose disposal in skeletal muscles, markedly decreased musclin mRNA expression (Fig. 3*C*) but not GLUT4 and myogenin (Supplemental Fig. 2*C*). Forskolin, which increases the intracellular cAMP contents similarly to epinephrine and isoproterenol, markedly and dose-dependently suppressed musclin mRNA expression (Fig. 3*D*) but not those of GLUT4 and myogenin (data not shown).

Finally, we assessed the biological role of musclin on insulin-stimulated glucose uptake and glycogen synthesis in differentiated C2C12 myocytes using recombinant musclin protein purified from media of stable C2C12 expressing FLAG-tagged musclin (Fig. 3, *E* and *F*). The cells were pretreated with 0.5 μg/ml recombinant musclin or FLAG peptide for 5 h and stimulated with phosphate-buffered saline or 100 nM insulin for 30 min (for 2-DG uptake) or 60 min (for glycogen synthesis). Treatment with insulin significantly increased 2-DG uptake and glycogen synthesis (Fig. 3, *E* and *F*). Musclin significantly attenuated insulin-stimulated 2-DG uptake (Fig. 3*E*) and glycogen synthesis at both basal and insulin-stimulated status (Fig. 3*F*). This 5-h treatment of musclin did not alter the expression levels of GLUT4, GLUT1, and hexokinase II mRNAs (data not shown).

DISCUSSION

Based on the hypothesis that skeletal muscles produce nutritionally regulated secretary factors, we identified musclin cDNA using an efficient SST technique. Although the precise physiological significance of musclin has yet to be determined, several important features were defined in the present study. *1*) Musclin protein is actively secreted; *2*) musclin mRNA is almost exclusively expressed in skeletal muscle; *3*) musclin mRNA expression is dynamically regulated by nutritional changes and hormonal factors, especially insulin; *4*) musclin mRNA expression is augmented in the skeletal muscle of obese insulin-resistant mice; and *5*) recombinant musclin inhibited insulin-stimulated glucose uptake and glycogen synthesis in myocytes. These observations suggest that musclin could func-

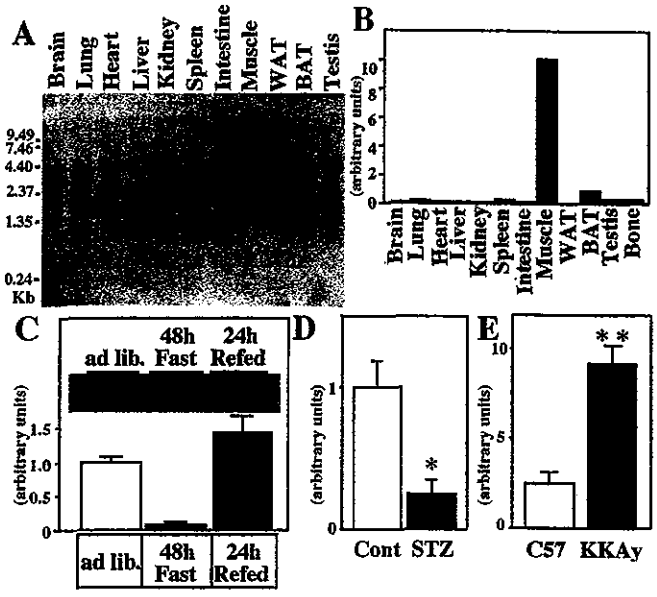

FIG. 2. ***In vivo* expression of musclin mRNA.** *A*, Northern blot analysis of musclin expression in mice. *B*, quantitative RT-PCR analysis of musclin mRNA expression in mice. *C*, regulation of musclin mRNA expression by nutritional status. Gastrocnemius muscles of mice fed *ad libitum*, fasted for 48 h, or fasted for 48 h and refed for 24 h (n = 5, each) were used for real-time RT-PCR. *Inset*, representative Northern blotting (n = 2, each). *D*, musclin mRNA expression in insulin-deficient STZ mice. Gastrocnemius muscles of STZ and control mice (n = 5, each) were subjected to real-time RT-PCR. The values were expressed relative to the level of 36B4 mRNA. *E*, musclin mRNA expression in KKAy mice. Gastrocnemius muscles of 13-week-old KKAy mice and age-matched C57BL/6J mice (n = 8, each) were used for real-time RT-PCR. The values were normalized to the level of cyclophilin mRNA. Data are mean ± S.E. values. *, $p < 0.05$; **, $p < 0.01$.

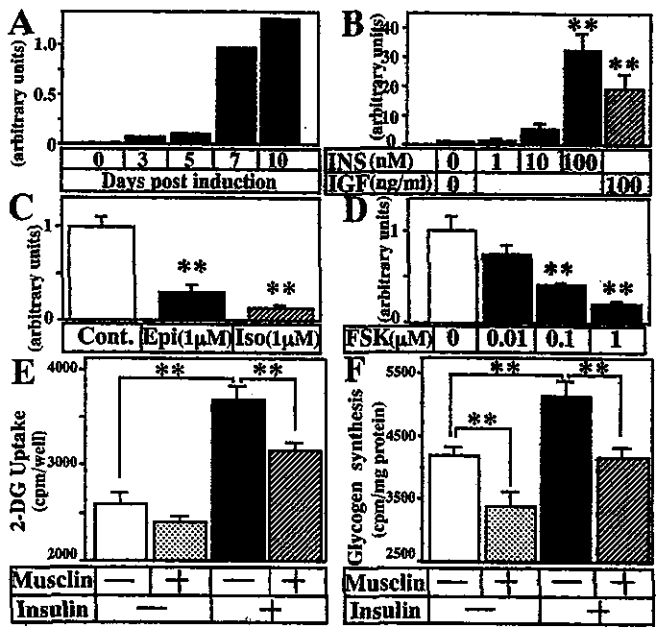

FIG. 3. **Regulation of musclin mRNA expression by various hormones and effects of musclin on insulin-stimulated glucose uptake and glycogen synthesis in C2C12 myocytes.** *A*, musclin mRNA expression during myocyte differentiation. C2C12 cells were harvested at the indicated days after differentiation induction for real-time PCR. *B–D*, regulation of musclin mRNA expression by insulin (*INS*), IGF-1 (*IGF*), epinephrine (*Epi*), isoproterenol (*Iso*), and forskolin (*FSK*) (real-time PCR). The expression level was expressed relative to that of cyclophlin mRNA (n = 3, each). *E* and *F*, effect of recombinant musclin on 2-DG uptake and glycogen synthesis. After 5-h pretreatment with FLAG peptide (0.5 μg/ml) as control or FLAG-tagged musclin (0.5 μg/ml), 2-DG uptake (*E*) and glycogen synthesis (*F*) were determined as described under "Experimental Procedures." Data are mean ± S.E. values (n = 6). **, $p < 0.01$. Similar results were obtained in two other independent experiments.

tion as an autocrine and paracrine factor in skeletal muscles and that increased production of musclin might be related to insulin resistance in the skeletal muscle of obese mice.

Musclin protein contained a homologous region to the functional 17 amino acids of the NP family, and basic KKKR sequence, a putative serine protease cleavage site. Proteins of the NP family are cleaved at this site and produce COOH-terminal active forms (12). Indeed, in cultures of mammalian cells transfected with musclin cDNA, full-length musclin protein and a trace amount of ^{76}KKKR^{79}-dependent cleaved form were secreted. Different from the NP family, the conserved 17 amino acids of musclin are not positioned between two cysteine residues, crucial for physiological protein folding to produce natriuretic activity. Therefore, it is unlikely that musclin has a natriuretic activity.

The size of the recombinant musclin protein purified from conditioned medium of mammalian cells expressing musclin cDNA was 15–20 kDa, although the recombinant protein extracted from *Escherichia coli* was 11 kDa (data not shown). This size difference suggests that musclin protein undergoes protein modification in mammalian cells. However, there is no distinct *N*-glycosylation site in musclin, and treatment with neuraminidase, which cuts out *O*-glycosylation, did not a produce size-different band in Western gel (date not shown), suggesting that musclin protein modification cannot be explained by typical glycosilation. Other possible forms of modifications including fatty acidation (*i.e.* grelin) (13) and amidation (*i.e.* adrenomedulin) (14) remain to be examined, since such modifications could be major regulators of the protein activity (13, 14).

We still do not know whether musclin is secreted into blood as an endocrine factor. Bruning *et al.* (6) reported that muscle-specific insulin receptor knock-out mice exhibited adipose hyperplasia and increased mass, suggesting insulin-mediated production of muscle-derived secretory factor that decreases adiposity. In preliminary experiments, we noted that adenovirus-mediated production of musclin protein in plasma significantly decreased fat mass in mice. Musclin could be the missing link from skeletal muscles to fat, receiving intense insulin regulation and controlling adiposity, although musclin mRNA expression was low in skinny STZ-treated mice and high in obese KKAy mice.

Conceivably, musclin may transmit important signal(s) to the skeletal muscle itself or to remote organs. Thus, establishment of a reliable method to measure musclin protein level in blood and knockout mice should enhance our understanding of the physiological significance of this muscle-derived secretory factor.

Acknowledgments—We thank the members of Shimomura's laboratory for helpful discussions and Drs. Nozomi Katayama, Hiroyuki Odaka, Yasuo Sugiyama (Takeda Chemical Industries, Ltd.), and Yasutomi Kamei (National instiute of Health and Nutrition, Japan) for helpful suggestions and reagents. We thank Dr. Shigekazu Nagata (Osaka University, Japan) for providing expression plasmid pEF-BOS.

Addendum—Thomas *et al.* (15) recently reported an osteoblast-derived factor, osteocrin, which was expressed in embryonic bone but disappeared after birth (15). The protein sequence of musclin seems to be identical to that of osteocrin. In our study, the expression level of musclin mRNA in skeletal muscle was more than 15-fold higher than in bones of 10–12-week-old mice (Fig. 2*B*) and more than 10-fold higher than in bones of 6-week-old rats (data not shown).

REFERENCES

1. Spiegelman, B. M., and Flier, J. S. (1996) *Cell* 87, 377–389
2. Shimomura, I., Funahashi, T., Takahashi, M., Maeda, K., Kotani, K., Nakamura, T., Yamashita, S., Miura, M., Fukuda, Y., Takemura, K., Tokunaga, K., and Matsuzawa, Y. (1996) *Nat. Med.* 2, 800–802
3. Zisman, A., Peroni, O. D., Abel, E. D., Michael, M. D., Mauvais-Jarvis, F.,

Lowell, B. B., Wojtaszewski, J. F., Hirshman, M. F., Virkamaki, A., Goodyear, L. J., Kahn, C. R., and Kahn, B. B. (2000) *Nat. Med.* **6**, 924–928
4. Hevener, A. L., He, W., Barak, Y., Le, J., Bandyopadhyay, G., Olson, P., Wilkes, J., Evans, R. M., and Olefsky, J. (2003) *Nat. Med.* **9**, 1491–1497
5. Norris, A. W., Chen, L., Fisher, S. J., Szanto, I., Ristow, M., Jozsi, A. C., Hirshman, M. F., Rosen, E. D., Goodyear, L. J., Gonzalez, F. J., Spiegelman, B. M., and Kahn, C. R. (2003) *J. Clin. Invest.* **112**, 608–618
6. Bruning, J. C., Michael, M. D., Winnay, J. N., Hayashi, T., Horsch, D., Accili, D., Goodyear, L. J., and Kahn, C. R. (1998) *Mol. Cell* **2**, 559–569
7. Kojima, T., and Kitamura, T. (1999) *Nat. Biotechnol.* **17**, 487–490
8. Nishizawa, H., Shimomura, I., Kishida, K., Maeda, N., Kuriyama, H., Nagaretani, H., Matsuda, M., Kondo, H., Furuyama, N., Kihara, S., Nakamura, T., Tochino, Y., Funahashi, T., and Matsuzawa, Y. (2002) *Diabetes* **51**, 2734–2741
9. Maeda, N., Shimomura, I., Kishida, K., Nishizawa, H., Matsuda, M., Nagaretani, H., Furuyama, N., Kondo, H., Takahashi, M., Arita, Y., Komuro, R., Ouchi, N., Kihara, S., Tochino, Y., Okutomi, K., Horie, M., Takeda, S., Aoyama, T., Funahashi, T., and Matsuzawa, Y. (2002) *Nat. Med.* **8**, 731–737
10. Mizushima, S., and Nagata, S. (1990) *Nucleic Acids Res.* **18**, 5322
11. Schmitz-Peiffer, C., Craig, D. L., and Biden, T. J. (1999) *J. Biol. Chem.* **274**, 24202–24210
12. Schmitt, M., Cockcroft, J. R., and Frenneaux, M. P. (2003) *Clin. Sci. (Lond.)* **105**, 141–160
13. Kojima, M., Hosoda, H., Date, Y., Nakazato, M., Matsuo, H., and Kangawa, K. (1999) *Nature* **402**, 656–660
14. Eto, T., Kitamura, K., and Kato, J. (1999) *Clin. Exp. Pharmacol. Physiol.* **26**, 371–380
15. Thomas, G., Moffatt, P., Salois, P., Gaumond, M. H., Gingras, R., Godin, E., Miao, D., Goltzman, D., and Lanctot, C. (2003) *J. Biol. Chem.* **278**, 50563–50571

nature medicine

Adiponectin-mediated modulation of hypertrophic signals in the heart

Rei Shibata[1,4], Noriyuki Ouchi[1,4], Masahiro Ito[2], Shinji Kihara[3], Ichiro Shiojima[1], David R Pimentel[2], Masahiro Kumada[3], Kaori Sato[1], Stephan Schiekofer[1], Koji Ohashi[3], Tohru Funahashi[3], Wilson S Colucci[2] & Kenneth Walsh[1]

Patients with diabetes and other obesity-linked conditions have increased susceptibility to cardiovascular disorders[1]. The adipocytokine adiponectin is decreased in patients with obesity-linked diseases[2]. Here, we found that pressure overload in adiponectin-deficient mice resulted in enhanced concentric cardiac hypertrophy and increased mortality that was associated with increased extracellular signal-regulated kinase (ERK) and diminished AMP-activated protein kinase (AMPK) signaling in the myocardium. Adenovirus-mediated supplemention of adiponectin attenuated cardiac hypertrophy in response to pressure overload in adiponectin-deficient, wild-type and diabetic *db/db* mice. In cultures of cardiac myocytes, adiponectin activated AMPK and inhibited agonist-stimulated hypertrophy and ERK activation. Transduction with a dominant-negative form of AMPK reversed these effects, suggesting that adiponectin inhibits hypertrophic signaling in the myocardium through activation of AMPK signaling. Adiponectin may have utility for the treatment of hypertrophic cardiomyopathy associated with diabetes and other obesity-related diseases.

Obesity is strongly associated with the metabolic syndrome, type 2 diabetes, hypertension and heart disease[1]. Pathological cardiac remodeling characterized by myocardial hypertrophy occurs with many obesity-related conditions[3,4], and diastolic dysfunction is one of the earliest clinical manifestations of insulin resistance[5]. But the molecular links between obesity and cardiac remodeling have not been clarified.

Adipose tissue can function as an endocrine organ by secreting adipocytokines that directly or indirectly affect obesity-linked disorders[6]. Adiponectin (also known as ACRP30) is a circulating adipose-derived cytokine that is downregulated in patients with obesity-linked diseases including type 2 diabetes, metabolic syndrome, coronary artery disease and hypertension[2,7]. Adiponectin-knockout (APN-KO) mice show diet-induced insulin resistance, increased intimal hyperplasia after acute vascular injury, and impaired angiogenic responses to ischemia[2,8–10]. Conversely, adiponectin overexpression reduces vascular lesions in a mouse model of atherosclerosis, and has vascular anti-inflammatory and proangiogenic effects. These data suggest that adiponectin acts as a modulator of obesity-linked vascular and metabolic disorders. But the role of adiponectin in the regulation of cardiac remodeling has not been examined previously.

To test the role of adiponectin in regulating cardiac hypertrophy, we subjected APN-KO mice to pressure overload caused by transverse aortic constriction (TAC). There were no significant differences in body weight or heart rate between APN-KO and wild-type mice after sham operation or TAC, and the increase in systolic blood pressure (sBP) after TAC was similar in wild-type and APN-KO mice (see **Supplementary Table 1** online). By gross morphologic examination 7 d after TAC, APN-KO mice (as compared to wild-type mice) had increased left ventricular wall thickness typical of exaggerated concentric hypertrophy (**Fig. 1a**). Echocardiographic measurements 7 d after TAC showed decreased left ventricular end-diastolic dimension (LVEDD) and increased interventricular septum (IVS) and left ventricular posterior wall thickness (LVPW) in APN-KO mice, as compared to wild-type animals (**Fig. 1b** and **Supplementary Table 1** online). The LVPW/LVEDD ratio increased markedly in APN-KO compared to wild-type mice after TAC, indicative of severe concentric hypertrophy. The calculated cardiac output was 14.1 ± 1.1, 16.2 ± 1.0, 14.0 ± 0.7 and 4.2 ± 0.2 ml/min in wild-type sham, wild-type TAC, APN-KO sham and APN-KO TAC, respectively. After TAC there was a small but statistically significant increase in heart weight/body weight ratio in APN-KO mice compared to wild-type animals (**Fig. 1c**). In addition, the increase in myocyte cross-sectional area in Masson trichrome–stained sections was greater in APN-KO than wild-type mice (**Fig. 1d**).

To confirm that the exaggerated hypertrophic response to pressure overload was a result of adiponectin deficiency, APN-KO and wild-type mice were treated with an adenoviral vector expressing adiponectin (Ad-APN) or with a control adenovirus (Ad-βgal), delivered through the jugular vein 3 d before TAC. At the time of surgery, adiponectin levels were 9.93 ± 1.08 μg/ml in wild-type control, 18.80 ± 1.02 μg/ml in wild-type Ad-APN, <0.05 μg/ml in APN-KO control and 11.10 ± 0.78 in APN-KO Ad-APN. Adiponectin is present in serum in trimer, hexamer or high molecular weight (HMW) forms[2]. The oligomer distribution of adenovirus-encoded adiponectin in the sera of APN-KO mice was similar to

[1]Molecular Cardiology/Whitaker Cardiovascular Institute, Boston University School of Medicine, 715 Albany Street, W611, Boston, Massachusetts 02118, USA. [2]Cardiovascular Medicine Section, Department of Medicine, Boston University Medical Center, and Myocardial Biology Unit, Boston University School of Medicine, 715 Albany Street, X704, Boston, Massachusetts 02118, USA. [3]Department of Internal Medicine and Molecular Science, Graduate School of Medicine, Osaka University, 2-2, Yamada-oka, Suita, Osaka, 565-0871, Japan. [4]These authors equally contributed to this work. Correspondence should be addressed to K.W. (kxwalsh@bu.edu).

Published online 21 November 2004; doi:10.1038/nm1137

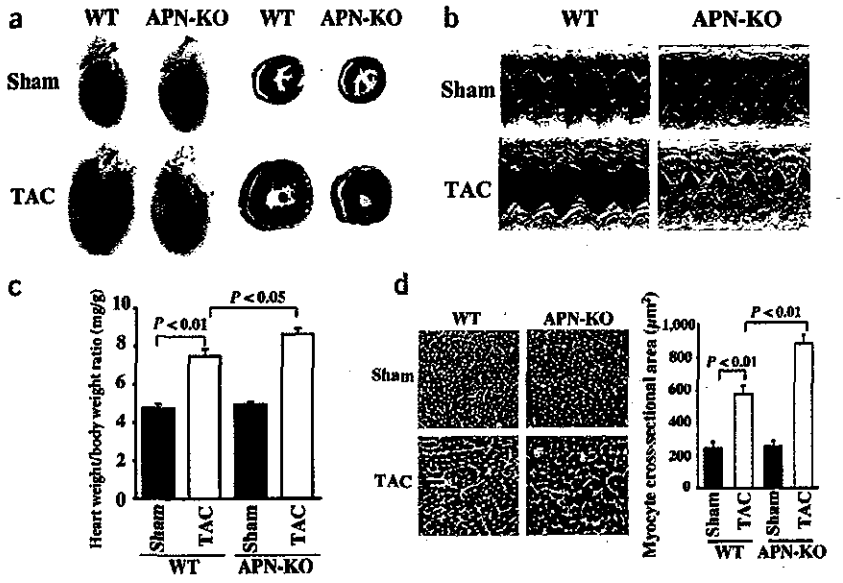

Figure 1 Enhanced pressure overload–induced cardiac hypertrophy in APN-KO mice subjected to TAC. (a) Representative pictures of hearts from wild-type (WT) and APN-KO mice at 7 d after sham operation or TAC (left). Representative hematoxylin and eosin-stained cross-sections of left ventricular myocardium from wild-type and APN-KO mice 7 d after sham operation or TAC (right). (b) Representative M-mode echocardiogram for APN-KO and wild-type (WT) mice 7 d after sham operation or TAC. (c) Heart weight/body weight ratio in wild-type ($n = 6$) and knockout mice ($n = 5$) 7 d after sham operation or TAC. (d) Histological analysis of heart sections from wild-type and APN-KO mice stained with Masson trichrome (magnification, x400; bar indicates 50 μm). Quantitative analysis of cardiac myocyte cross-sectional area ($n = 200$ per section) in wild-type ($n = 6$) and APN-KO mice ($n = 5$). Results are presented as mean ± s.e.m.

that of endogenous adiponectin in wild-type mice as determined by gel filtration analysis (Fig. 2a). Ad-APN treatment attenuated the TAC-induced changes in left ventricular morphology (increased IVS, increased LVPW) observed in APN-KO mice (Fig. 2b). Ad-APN also decreased heart weight/body weight ratio and myocyte cross-sectional area in this model (Fig. 2c). Mortality at 6, 7 and 14 d after TAC was higher in APN-KO compared to wild-type mice (Fig. 2d), presumably as a result of the notable decrease in cardiac output after TAC in APN-KO mice.

Ad-APN treatment also attenuated the increased IVS and LVPW response to TAC in *db/db* mice, which lack a functional leptin receptor, a model of obesity and diabetes (Fig. 2e). Finally, APN-KO mice subjected to angiotensin II (AngII) infusion exhibited increased IVS and LVPW compared to AngII-infused wild-type mice (Fig. 2f). The increase in sBP after AngII infusion was similar in wild-type and APN-KO mice (130.8 ± 2.4 mmHg in wild-type versus 134.4 ± 3.1 mmHg in APN-KO mice). Ad-APN treatment attenuated the AngII-induced changes in left ventricular morphology observed in both the APN-KO and wild-type mice (Fig. 2f). Thus, adiponectin supplementation was antihypertrophic in several models of pathological heart growth.

To examine the effects of adiponectin in cardiac myocytes at the cellular level, ventricular myocytes obtained from rats were subjected to α-adrenergic receptor (αAR) stimulation with norepinephrine in the presence of propranolol (Pro)[11], with or without the addition of recombinant adiponectin protein. αAR stimulation for 48 h caused an increase in myocyte size and protein synthesis that was associated with reorganization of sarcomeric actin (Fig. 3a,b), and these effects were prevented by pretreatment with adiponectin. Adiponectin alone had no effect on myocyte size, protein synthesis or actin organization. Adiponectin treatment also suppressed AngII-stimulated myocyte hypertrophy (data not shown).

Gq-dependent activation of ERK is an important mediator of myocyte hypertrophy in response to pressure overload[12] and αAR stimulation[11]. Therefore, the effect of adiponectin on ERK phosphorylation at Thr202 and Tyr204 was investigated by western blotting. *In vivo*, ERK phosphorylation was similar in myocardium from sham-operated APN-KO and wild-type mice, whereas pressure overload-induced ERK phosphorylation was enhanced in APN-KO compared to wild-type mice (Fig. 3c). In cultured cardiac myocytes, αAR stimulation induced ERK phosphorylation that was suppressed by pretreatment with adiponectin (Fig. 3d). Under the conditions of these assays, treatment with the MEK inhibitor U0126 reduced αAR-induced hypertrophy by 82% ($P < 0.01$ versus control), indicating that ERK inhibition by adiponectin contributes to the suppression of cardiac myocyte hypertrophy. Adiponectin treatment alone had no effect on ERK phosphorylation in cardiac myocytes. Adiponectin treatment also suppressed AngII-stimulated ERK phosphorylation (data not shown). The trimer form specifically suppressed αAR-stimulated ERK phosphorylation, whereas the hexamer or HMW forms of adiponectin had little effect (Fig. 3e). The trimer form of adiponectin also blocked the increase in myocyte size caused by αAR stimulation (data not shown). In contrast, the HMW form of adiponectin appears to be specific for its vascular-protective actions[13].

Because adiponectin functions to induce AMPK signaling in many cell types including skeletal muscle, liver, adipocytes and endothelial cells[14–17], the phosphorylation of AMPK at Thr172 of its α subunit was assessed by western blotting. Treatment with a physiological concentration of adiponectin stimulated the phosphorylation of AMPK in cultured cardiac myocytes in a time-dependent manner (Fig. 4a). Among the three oligomeric forms of adiponectin, only the trimer stimulated AMPK phosphorylation (Fig. 4b). Conversely, AMPK phosphorylation was attenuated in APN-KO compared to wild-type hearts in both sham operation and TAC conditions (Fig. 4c). To test whether AMPK is involved in the inhibitory effects of adiponectin on myocyte hypertrophy, cultured cardiac myocytes were transduced with an adenoviral vector expressing a c-Myc-tagged dominant-negative mutant of AMPK (Ad-dnAMPK). Transduction with Ad-dnAMPK suppressed adiponectin-induced AMPK phosphorylation and acetyl-CoA carboxylase (ACC) phosphorylation (Fig. 4d). Quantitative measurements of multiple blots revealed that Ad-dnAMPK reduced AMPK and ACC phosphorylation by 97% and 90%, respectively, at the 60-min time point ($P < 0.01$ versus control). Transduction with Ad-dnAMPK also prevented the inhibitory effect of exogenous adiponectin on αAR-stimulated myocyte hypertrophy and ERK phosphorylation (Fig. 4e,f). Ad-dnAMPK alone had no effect on myocyte size, protein synthesis or ERK phosphorylation. Collectively, these data suggest that adiponectin exerts its inhibitory effect on hypertrophic signaling through activation of AMPK.

The present study shows that the fat-derived factor adiponectin can modulate cardiac remodeling. Concentric hypertrophy and diastolic

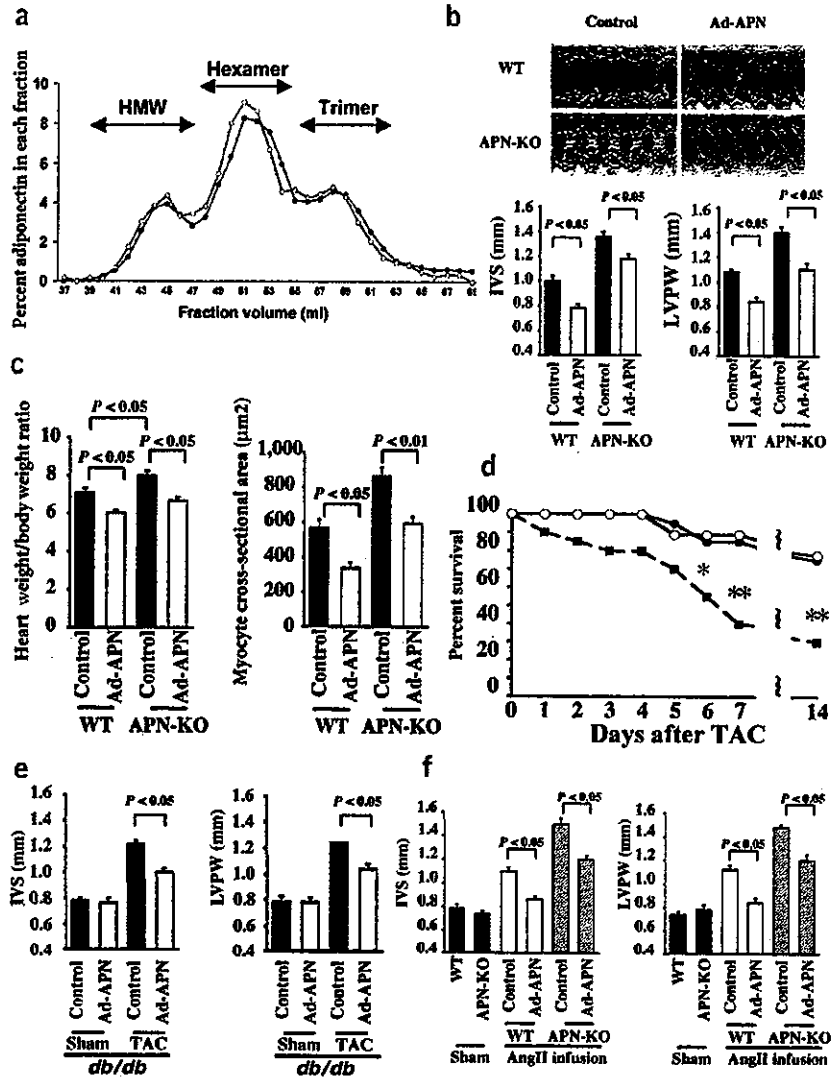

Figure 2 Adenovirus-mediated supplementation of adiponectin protects against the development of cardiac hypertrophy. (**a**) Oligomeric state of adenovirus-delivered adiponectin in APN-KO mouse (open circle) and endogenous adiponectin in wild-type mouse (closed circles) assessed by gel filtration analysis. The adenoviral vector expressing adiponectin (Ad-APN, 2 x 10^8 p.f.u. total) was delivered through the jugular vein, and the oligomeric state of adiponectin was analyzed 3 d after Ad-APN injection. (**b**) Adenovirus-mediated supplementation of adiponectin in APN-KO and wild-type (WT) mice attenuated cardiac hypertrophy in response to TAC as shown by echocardiography. Adenoviral vectors expressing adiponectin (Ad-APN, 2 x 10^8 p.f.u. total, $n = 3$) or β-galactosidase (control, $n = 3$) were delivered intravenously through the jugular vein 3 d before TAC surgery. Left ventricular wall thickness (IVS and LVPW) was determined at 3 d after TAC. (**c**) Heart weight/body weight ratio and cardiac myocyte cross-sectional area in wild-type ($n = 5$) and knockout mice ($n = 3$) treated with Ad-APN or Ad-βgal (control) were determined at 7 d after sham operation or TAC. (**d**) Decreased survival of APN-KO mice (closed squares) after TAC ($n = 20$; $^*P < 0.05$, $^{**}P < 0.01$) in comparison with wild-type mice (closed circles) after TAC ($n = 20$). Adenovirus-mediated supplementation of adiponectin in APN-KO ($n = 9$) (open circles) improved survival to a level that is comparable to that of wild-type mice. (**e**) Adenovirus-mediated supplementation of adiponectin in diabetic *db/db* mice attenuated cardiac hypertrophy in response to TAC as shown by echocardiography. Ad-APN (2 x 10^8 p.f.u. total, $n = 4$) or β-galactosidase (control, $n = 4$) were delivered intravenously through the jugular vein 3 d before TAC surgery. Wall thickness (IVS and LVPW) was determined at 3 d after TAC surgery or sham operation. (**f**) APN-KO mice showed an increased cardiac hypertrophy following AngII infusion relative to wild-type mice ($n = 4$). Adenovirus-mediated supplementation of adiponectin (2 x 10^8 p.f.u.) in APN-KO ($n = 4$) and wild-type ($n = 4$) mice attenuated AngII-induced cardiac hypertrophy. Wall thickness (IVS and LVPW) was determined after 14 d of AngII infusion. Results are presented as mean ± s.e.m.

dysfunction are frequently observed in diabetes and other obesity-related disorders that are associated with hypoadiponectinemia[2–5]. The findings reported here suggest that hypoadiponectinemia may contribute to the development of pathologic cardiac hypertrophy in such patients, and that procedures to restore or increase plasma adiponectin levels could potentially be beneficial for the prevention of pathological cardiac remodeling in disorders associated with obesity.

The ability of adiponectin to attenuate cardiac hypertrophy is likely due to its ability to stimulate AMPK-dependent signaling within cardiac myocytes[18]. AMPK is a stress-activated protein kinase that participates in the regulation of energy and metabolic homeostasis[19–21]. AMPK activity is increased during acute and chronic stresses such as hypoxia, ischemia and cardiac hypertrophy[19–22]. Adiponectin can also stimulate AMPK signaling in endothelial cells[13,17], but no difference in capillary density was seen between wild-type and APN-KO hearts after TAC (data not shown), suggesting that changes in myocyte signaling mediate the cardioprotective actions of adiponectin. In cardiac myocytes, adiponectin-stimulated AMPK activation suppressed ERK activation, an important prohypertrophic signaling step[11,12,23]. These observations suggest that the adiponectin-AMPK signaling axis serves as a functional link between adipose tissue and the heart, and thereby influences the extent of cardiac remodeling in obesity-linked conditions.

METHODS

Materials. Phospho-AMPK (Thr172), pan-α-AMPK and phospho-p42/44 ERK (Thr202/Tyr204) and total ERK antibodies and U0126 were purchased from Cell Signaling Technology. Tubulin antibody was from Oncogene. Phospho-ACC (Ser79), ACC and c-Myc tag antibody were purchased from Upstate Biotechnology. L-norepinephrine, DL-propranolol and AngII were purchased from Sigma. Recombinant mouse adiponectin was prepared as described previously[17]. Adenovirus vectors containing the gene for β-galactosidase (Ad-βgal), full-length mouse adiponectin (Ad-APN), and dominant-negative AMPKα2 (Ad-dnAMPK) were prepared as described previously[8,19]. The trimer, hexamer and HMW forms of adiponectin were prepared as described previously[13].

Transverse aortic constriction. We used adiponectin knockout (APN-KO), wild-type and *db/db* mice in a C57/BL6 background[8]. Study protocols were approved by the Institutional Animal Care and Use Committee at Boston University. Mice, at the ages of 7–11 weeks, were anesthetized with sodium pentobarbital (50 mg/kg intraperitoneally). The chest was opened, and following

blunt dissection through the intercostal muscles, the thoracic aorta was identified. A 7-0 silk suture was placed around the transverse aorta and tied around a 26-gauge blunt needle, which was subsequently removed[24]. Sham-operated mice underwent a similar surgical procedure without constriction of the aorta. After 7 d, we subjected surviving mice to transthoracic echocardiography and cardiac catheterization to determine heart rate and proximal aortic pressure. Animals were then killed and the hearts were weighed.

Adenovirus-mediated gene transfer. We injected 2×10^8 plaque-forming units (p.f.u.) of Ad-APN or Ad-βgal into the jugular vein of mice 3 d prior to TAC. We performed echocardiography 3 d after surgery. We determined mouse adiponectin levels by ELISA kit (Otsuka Pharmaceutical Co. Ltd.). The oligomeric state of adiponectin was analyzed by gel filtration chromatography as described previously[13].

AngII infusion. We subcutaneously infused AngII (3.2mg/kg/d) into APN-KO and wild-type mice using an implanted osmotic minipump (Durect Corporation). We transduced some mice with 2×10^8 p.f.u. of Ad-APN or Ad-βgal injected into the jugular vein. After 14 d, mice were subjected to transthoracic echocardiography and cardiac catheterization to determine heart rate and blood pressure.

Echocardiography. To measure left ventricular wall thickness and chamber dimensions, we performed echocardiography with an Acuson Sequoia C-256 machine using a 15-MHz probe. After we obtained a two-dimensional image, we measured M-mode images of the left ventricular posterior wall thickness. We calculated cardiac output by the cubed method ($1.047 \times (LVEDD^3 - LVESD^3) \times$ heart rate).

Cell culture and adenoviral infection. Primary cultures of the neonatal rat ventricular myocytes were prepared as described previously[23]. The isolated myocytes were cultured in Dulbecco Modified Eagle medium containing 7% fetal calf serum. Before each experiment, we placed cells in serum-free Dulbecco Modified Eagle medium for 24 h. For the adiponectin stimulation studies, we treated with 30 μg/ml of mouse recombinant adiponectin for the indicated lengths of time. Experiments for norepinephrine stimulation were performed by treating cells with 30 μg/ml of mouse recombinant adiponectin or vehicle for 30 min. We then treated cells with 2 μM of propranolol for 30 min and stimulated with 1 μM norepinephrine for the indicated lengths of time. In some experiments, we infected the cells with Ad-βgal and Ad-dnAMPK at a multiplicity of infection of 50 for 24 h before treatments. Myocyte surface area was assessed using semi-automatic computer-assisted planimetry (Bioquant) from two-dimensional images of unstained cells. [^{3}H]-leucine incorporation was determined as previously described[24].

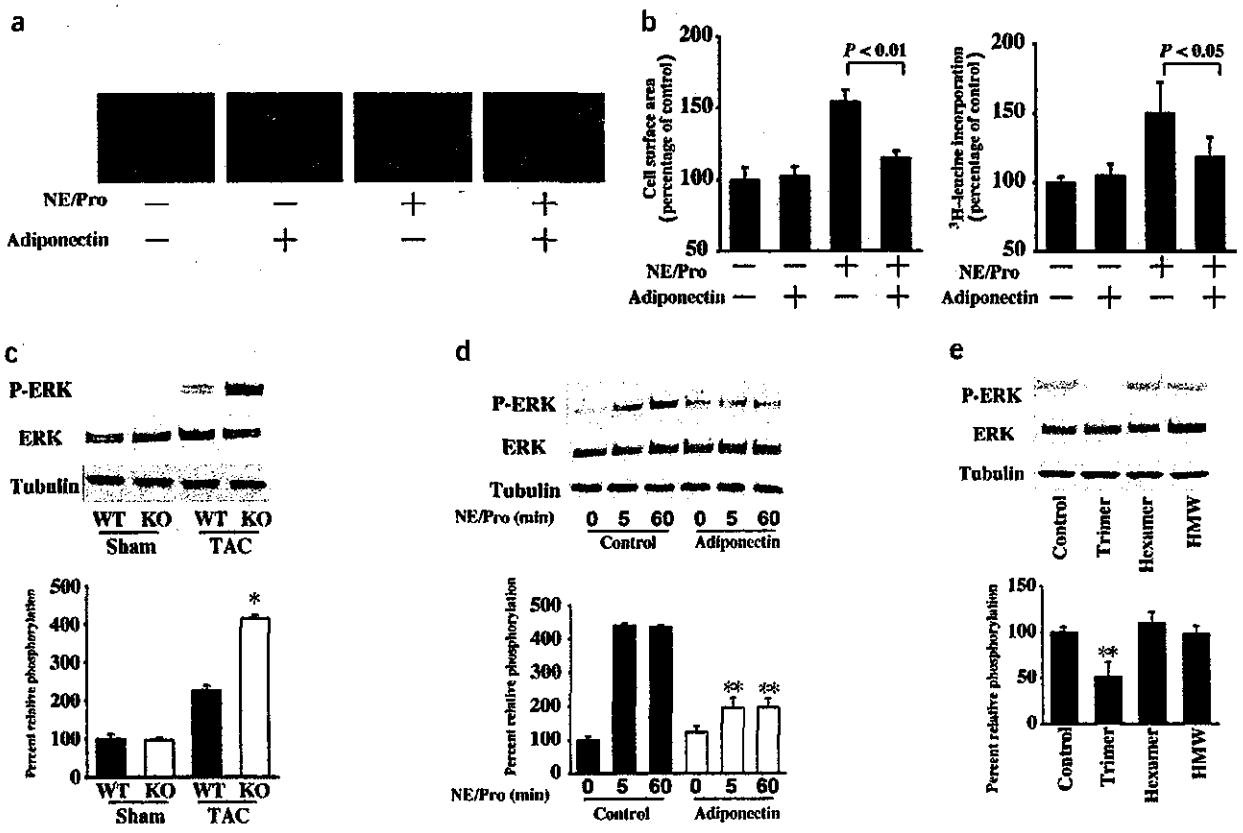

Figure 3 Adiponectin inhibits the hypertrophic response to αAR stimulation or pressure overload. (a) Representative example of immunostaining of sarcomeric F-actin with rhodamine phalloidin in rat cardiac myocytes. Cells were pretreated with adiponectin (30 μg/ml) or vehicle for 30 min, Pro (2 μM) for an additional 30 min, followed by the addition of norepinephrine (NE) for 48 h. (b) Quantitative analysis of cell surface area measured by semi-automatic computer-assisted planimetry (Bioquant) from two-dimensional images of 100 cells selected at random (left) and protein synthesis measured by [^{3}H]-leucine incorporation (right). (c) The phosphorylation (P-) of ERK in heart tissues from wild-type and APN-KO mice at 7 d after sham operation or TAC. (d) Effect of adiponectin on the phosphorylation of ERK in response to αAR-stimulation in cultured rat cardiac myocytes. Cells were pretreated with adiponectin (30 μg/ml) or vehicle for 30 min, 2 μM Pro for an additional 30 min and then stimulated with or without 1 μM norepinephrine (NE) for the indicated length of time. (e) Effects of three different oligomeric forms of adiponectin on the phosphorylation of ERK in response to αAR-stimulation in cultured rat cardiac myocytes. Cells were pretreated with each form of adiponectin (5 μg/ml) or vehicle for 30 min, 2 μM Pro for an additional 30 min and then stimulated with 1 μM NE for 5 min. Relative phosphorylation levels of ERK were quantified using the US National Institutes of Health image program. Immunoblots were normalized to total loaded protein. Results are presented as mean ± s.d. ($n = 3$–6). $^*P < 0.05$ versus wild-type. $^{**}P < 0.05$ versus control.

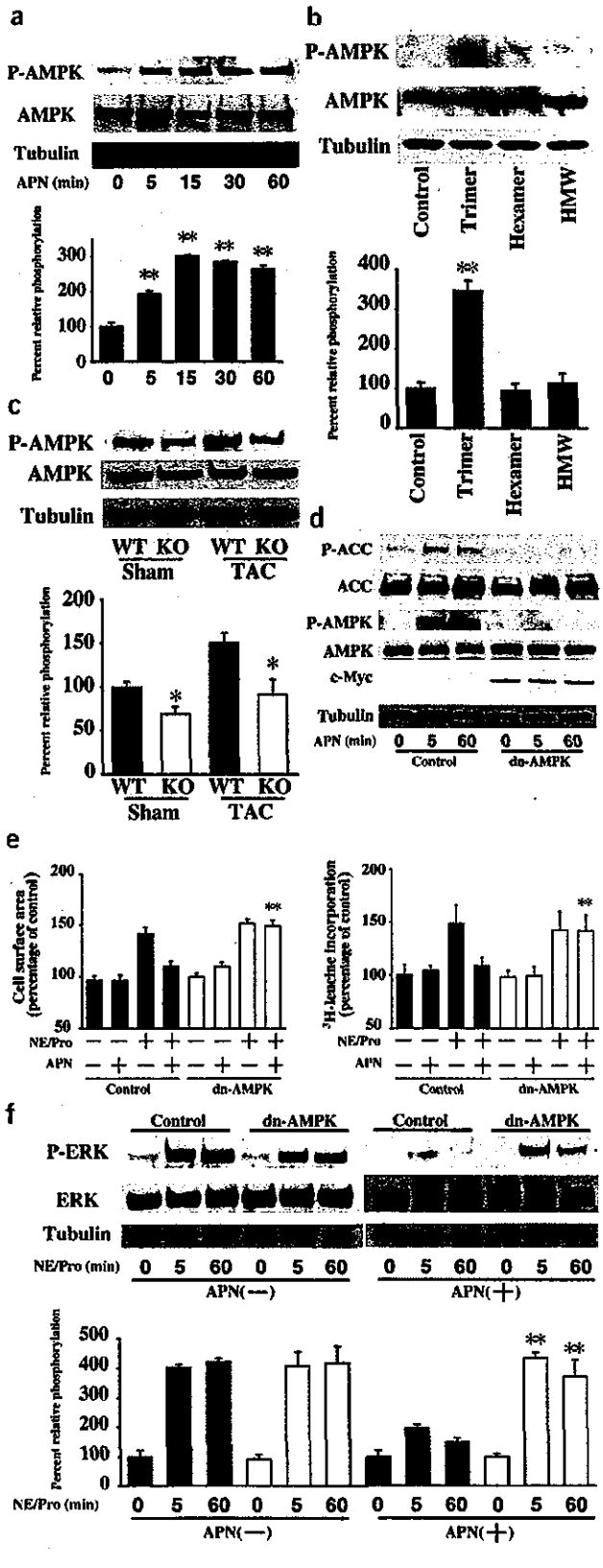

Figure 4 Adiponectin inhibition αAR-stimulated myocyte hypertrophy is mediated through AMPK signaling. (**a**) Time-dependent changes in the phosphorylation of AMPK in rat cultured cardiac myocytes after adiponectin treatment (30 μg/ml). (b) Effects of three different oligomeric forms of adiponectin (5 μg/ml) on the phosphorylation of AMPK. (**c**) The phosphorylation of AMPK in myocardium from wild-type (WT) and APN-KO mice at 7 d after sham operation or TAC. (**d**) Ad-dnAMPK reversed adiponectin stimulation of AMPK and ACC phosphorylation. Rat cardiac myocytes were transduced with c-Myc-tagged Ad-dnAMPK or Ad-βgal (control) at a multiplicity of infection of 50 for 24 h in serum-starved media. Cells were treated with adiponectin (30 μg/ml) for the indicated lengths of time. (**e**) Contribution of AMPK signaling to the inhibitory effect of adiponectin on αAR-stimulated myocyte hypertrophy. After 24-h transduction of rat cardiac myocytes with Ad-dnAMPK or Ad-βgal (control), cells were pretreated with adiponectin (30 μg/ml) or vehicle for 30 min and then treated with 2 μM Pro for 30 min and stimulated with or without 1 μM norepinephrine (NE) for 48 h. Quantitative analysis of cell surface area was performed in 100 randomly selected cells (left) or ^{3}H-leucine incorporation into protein (right). (**f**) Effect of Ad-dnAMPK on adiponectin inhibition of NE/Pro-induced ERK phosphorylation. Cells were treated as in e and then stimulated with or without 1 μM norepinephrine (NE) for the indicated lengths of time. Relative phosphorylation levels of AMPK and ERK were quantified using the US National Institutes of Health image program. Immunoblots were normalized to total loaded protein. Results are presented as mean ± s.d. (n = 3–5). $^*P < 0.05$ versus wild-type. $^{**}P < 0.05$ versus control.

Immunohistochemical analysis. Mice were killed and left ventricular tissue was obtained 7 d after TAC. We embedded tissue in OCT compound (Miles) and snap-froze it in liquid nitrogen. We then prepared tissue slices (5 μm). Tissue sections were stained with hematoxylin and eosin or with Masson trichrome. We calculated the myocyte cross-sectional area by measuring 200 cells per section. To determine sarcomeric F-actin organization, we stained cultured myocytes with FITC-conjugated phalloidin (Sigma).

Western blot analysis. Heart tissue samples obtained on day 7 after surgery were homogenized in lysis buffer containing 20 mM Tris-HCl (pH 8.0), 1% NP-40, 150 mM NaCl, 0.5% deoxycholic acid, 1 mM sodium orthovanadate, and protease inhibitor cocktail (Sigma). We homogenized rat myocytes in the same lysis buffer. Protein (50 μg) was separated with denaturing SDS 10% polyacrylamide gels. After transfer of protein to membranes, we performed immunoblot analysis with the indicated antibodies at a 1:1,000 dilution. This was followed by incubation with secondary antibody conjugated with horseradish peroxidase at a 1:5,000 dilution. We used the ECL Western Blotting Detection kit (Amersham Pharmacia Biotech) for detection.

Statistical analysis. Data are presented as mean ± s.e.m. or s.d. as indicated in the figure legends. Statistical analysis was performed by student's t-test, Scheffe's F test and χ^2 analysis. A value of $P < 0.05$ was accepted as statistically significant.

Note: Supplementary information is available on the Nature Medicine website.

ACKNOWLEDGMENTS

We acknowledge the technical assistance of S. Tanaka and A. Bialik. This work was supported by US National Institutes of Health (NIH) grants HL66957, AR40197, AG15052 and AG17241 to K. Walsh, HL61639 and HL20612 to W.S. Colucci, NIH Cardiovascular Scientist Training Grant HL07224 to D.R. Pimentel; and grants from the Japanese Ministry of Education and the Japan Society for Promotion of Science-Research for the Future Program. R. Shibata, N. Ouchi and M. Ito were supported by grants from the Uehara Memorial Foundation.

COMPETING INTERESTS STATEMENT

The authors declare that they have no competing financial interests.

Received 23 June; accepted 18 October 2004
Published online at http://www.nature.com/naturemedicine/

1. Reilly, M.P. & Rader, D.J. The metabolic syndrome: more than the sum of its parts? *Circulation* **108**, 1546–1551 (2003).
2. Ouchi, N., Kihara, S., Funahashi, T., Matsuzawa, Y. & Walsh, K. Obesity, adiponectin and vascular inflammatory disease. *Curr. Opin. Lipidol.* **14**, 561–566 (2003).
3. Ilercil, A. *et al.* Relationship of impaired glucose tolerance to left ventricular structure and function: The Strong Heart Study. *Am. Heart J.* **141**, 992–998 (2001).
4. Rutter, M.K. *et al.* Impact of glucose intolerance and insulin resistance on cardiac structure and function: sex-related *differences in* the Framingham Heart Study. *Circulation* **107**, 448–454 (2003).
5. Schannwell, C.M., Schneppenheim, M., Perings, S., Plehn, G. & Strauer, B.E. Left ventricular diastolic dysfunction as an early manifestation of diabetic cardiomyopathy. *Cardiology* **98**, 33–39 (2002).
6. Kahn, B.B. & Flier, J.S. Obesity and insulin resistance. *J. Clin. Invest.* **106**, 473–481 (2000).
7. Scherer, P.E., Williams, S., Fogliano, M., Baldini, G. & Lodish, H.F. A novel serum protein similar to C1q, produced exclusively in adipocytes. *J. Biol. Chem.* **270**, 26746–26749 (1995).
8. Maeda, N. *et al.* Diet-induced insulin resistance in mice lacking adiponectin/ACRP30. *Nat. Med.* **8**, 731–737 (2002).
9. Kubota, N. *et al.* Disruption of adiponectin causes insulin resistance and neointimal formation. *J. Biol. Chem.* **277**, 25863–25866 (2002).
10. Shibata, R. *et al.* Adiponectin stimulates angiogenesis in response to tissue ischemia through stimulation of amp-activated protein kinase signaling. *J. Biol. Chem.* **279**, 28670–28674 (2004).
11. *Xiao, L. et al.* MEK1/2–ERK1/2 mediates alpha1-adrenergic receptor-stimulated hypertrophy in adult rat ventricular myocytes. *J. Mol. Cell. Cardiol.* **33**, 779–787 (2001).
12. Esposito, G. *et al.* Cardiac overexpression of a G(q) inhibitor blocks induction of extracellular signal-regulated kinase and c-Jun NH(2)-terminal kinase activity in *in vivo* pressure overload. *Circulation* **103**, 1453–1458 (2001).
13. Kobayashi, H. *et al.* Selective suppression of endothelial cell apoptosis by the high molecular weight form of adiponectin. *Circ. Res.* **94**, e27–e31 (2004).
14. Tomas, E. *et al.* Enhanced muscle fat oxidation and glucose transport by ACRP30 globular domain: acetyl-CoA carboxylase inhibition and AMP-activated protein kinase activation. *Proc. Natl. Acad. Sci. USA* **99**, 16309–16313 (2002).
15. Yamauchi, T. *et al.* Adiponectin stimulates glucose utilization and fatty-acid oxidation by activating AMP-activated protein kinase. *Nat. Med.* **8**, 1288–1295 (2002).
16. Wu, X. *et al.* Involvement of AMP-activated protein kinase in glucose uptake stimulated by the globular domain of adiponectin in primary rat adipocytes. *Diabetes* **52**, 1355–1363 (2003).
17. *Ouchi, N. et al.* Adiponectin stimulates angiogenesis by promoting cross-talk between AMP-activated protein kinase and Akt signaling in endothelial *cells. J. Biol. Chem.* **279**, 1304–1309 (2004).
18. Chan, A.Y., Soltys, C.L., Young, M.E., Proud, C.G. & Dyck, J.R. Activation of AMP-activated protein kinase inhibits protein synthesis associated with hypertrophy in the cardiac myocyte. *J. Biol. Chem.*, **279**, 32771–32179 (2004).
19. Nagata, D., Mogi, M. & Walsh, K. AMP-activated protein kinase (AMPK) signaling in endothelial cells is essential for angiogenesis in response to hypoxic stress. *J. Biol. Chem.* **278**, 31000–31006 (2003).
20. Mu, J., Brozinick, J.T., Jr, Valladares, O., Bucan, M. & Birnbaum, M.J. A role for AMP-activated protein kinase in contraction- and hypoxia-regulated glucose transport in skeletal muscle. *Mol. Cell* **7**, 1085–1094 (2001).
21. Kudo, N., Barr, A.J., Barr, R.L., Desai, S. & Lopaschuk, G.D. High rates of fatty acid oxidation during reperfusion of ischemic hearts are associated with a decrease in malonyl-CoA levels due to an increase in 5'-AMP-activated protein kinase inhibition of acetyl-CoA carboxylase. *J. Biol. Chem.* **270**, 17513–17520 (1995).
22. Tian, R., Musi, N., D'Agostino, J., Hirshman, M.F. & Goodyear, L.J. Increased adenosine monophosphate-activated protein kinase activity in rat hearts with pressure-overload hypertrophy. *Circulation* **104**, 1664–1669 (2001).
23. Pimentel, D.R. *et al.* Reactive oxygen species mediate amplitude-dependent *hypertrophic* and apoptotic responses to mechanical stretch in cardiac myocytes. *Circ. Res.* **89**, 453–460 (2001).
24. Rogers, J.H. *et al.* RGS4 causes increased mortality and reduced cardiac hypertrophy in response to pressure overload. *J. Clin. Invest.* **104**, 567–576 (1999).

Circ J 2004; **68:** 975–981

Adiponectin as a Biomarker of the Metabolic Syndrome

Miwa Ryo, MD; Tadashi Nakamura, MD; Shinji Kihara, MD; Masahiro Kumada, MD; Satomi Shibazaki, MD*; Mihoko Takahashi, PhD*; Masaki Nagai, MD*; Yuji Matsuzawa, MD**; Tohru Funahashi, MD

Background The metabolic syndrome, a cluster of abdominal obesity, dyslipidemia, hypertension and hyperglycemia, is a common basis for atherosclerotic vascular diseases in industrial countries exposed to overnutrition. Adiponectin is an adipose-derived plasma protein with anti-atherogenic and insulin-sensitizing activities.
Methods and Results A total of 661 Japanese adults (479 men, 53±10 years; 182 women 56±10 years) were enrolled. Plasma adiponectin concentrations correlated negatively with waist circumference, visceral fat area, serum triglyceride concentration, fasting plasma glucose, fasting plasma insulin, and systolic and diastolic blood pressure in both sexes. A positive correlation was found between plasma adiponectin and high-density lipoprotein cholesterol concentrations in both sexes. The mean number of components of the metabolic syndrome increased as the plasma adiponectin concentration decreased: 2.57±1.34 for men and 2.00±1.51 for women with adiponectin concentrations <4.0μg/ml. In all, 52.3% of men and 37.5% of women with adiponectin concentrations <4.0μg/ml fulfilled the criteria for metabolic syndrome.
Conclusion Hypoadiponectinemia is closely associated with the clinical phenotype of the metabolic syndrome and measuring the plasma concentration of adiponectin may be useful for management of the metabolic syndrome. (*Circ J* 2004; **68:** 975–981)

Key Words: Adipocytokine; Adiponectin; Hypoadiponectinemia; Metabolic syndrome; Visceral fat

An elevated plasma concentration of low-density lipoprotein (LDL)-cholesterol is one of the major risk factors for the development of coronary artery disease (CAD). Clinical trials have demonstrated that LDL-lowering therapy can reduce major coronary events and coronary mortality.[1] A secondary target for the prevention of CAD beyond cholesterol-lowering therapy is management of the metabolic syndrome, which comprises a cluster of cardiovascular risk factors, including abdominal obesity, dyslipidemia, glucose intolerance and hypertension. Although genetic factors may be involved, it has been generally accepted that accumulation of excess body fat, particularly abdominal obesity or intra-abdominal visceral obesity caused by overnutrition and physical inactivity, promotes the development of the metabolic syndrome.[2–8]

Recent research has demonstrated that adipose tissue produces and secretes various bioactive substances, conceptualized as adipocytokines, and their dysregulation in abdominal or visceral obesity may participate in the development of the metabolic syndrome.[9–11] For example, overproduction of plasminogen activator inhibitor type 1 in excess visceral fat inhibits the fibrinolytic system and consequently may lead to thrombotic vascular disorders.[11] Adiponectin is an adipose-specific plasma protein, which we identified in the human adipose cDNA project.[12] Adiponectin suppresses almost all processes involved in atherosclerotic vascular change, including the expression of adhesion molecules in vascular endothelial cells,[13,14] proliferation of vascular smooth muscle cells,[15] and formation of foam cells in vitro,[16] and it exhibits anti-atherosclerotic activity in vivo.[17] However, low plasma adiponectin concentrations are found in obese subjects.[18] We and others have also demonstrated that adiponectin has insulin-sensitizing activity, and that high plasma adiponectin is a negative risk factor for type 2 diabetes in diabetes-prone people.[19–21] Recent studies have shown that adiponectin is related to endothelium-dependent vasodilatation and its plasma concentrations are low in subjects with essential hypertension.[22] These clinical and experimental data suggest that adiponectin may play a significant role in the development of the metabolic syndrome.

The significance of plasma adiponectin measurement in subjects with the metabolic syndrome has not been well studied. In the present study, we measured it in a large Japanese population and investigated the relationship between plasma adiponectin concentration and the metabolic syndrome.

Methods

Subjects

The study group comprised 661 Japanese adult subjects [mean age±SD, 54±10 years, range: 20–78 years; 479 men (53±10 years), 182 women (56±10 years)]. To investigate the prevalence of the metabolic syndrome and the range of plasma adiponectin concentrations in the general Japanese population, 577 cases [438 men (54±9 years), 139 women (55±8 years)], who underwent health examination in the institutions that participated in the Japanese Visceral Fat Syndrome (J-VFS) Study Committee of the Ministry of

(Received June 14, 2004; revised manuscript received August 9, 2004; accepted August 23, 2004)
*Department of Internal Medicine and Molecular Science, Graduate School of Medicine, Osaka University, Suita, Osaka, *Department of Public Health, Saitama Medical School, Saitama and **Sumitomo Hospital, Osaka, Japan*
Mailing address: Tohru Funahashi, MD, PhD, Department of Internal Medicine and Molecular Science, Graduate School of Medicine, Osaka University, 2-2 Yamadaoka, Suita, Osaka 565-0871, Japan. E-mail: tohru@imed2.med.osaka-u.ac.jp

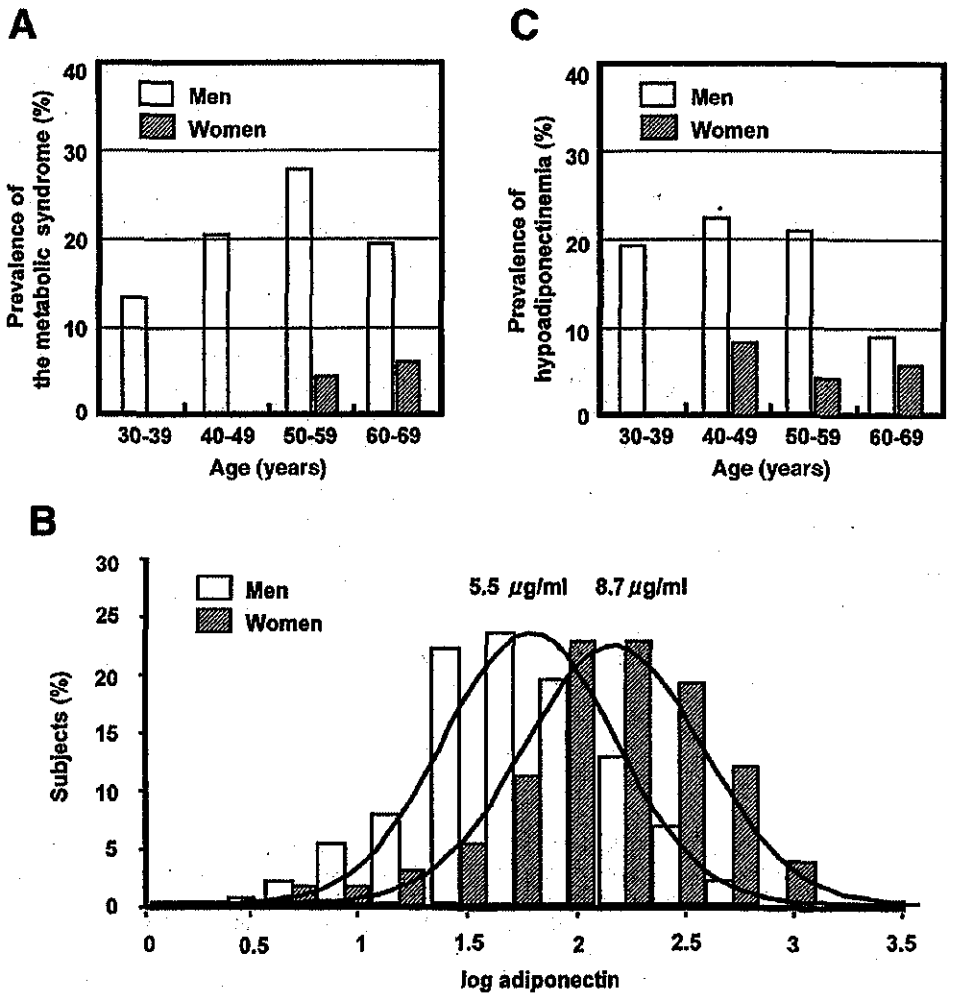

Fig 1. (A) Age-specific prevalence of the metabolic syndrome. (B) Percentages of subjects according to log adiponectin concentrations. Logarithmic transformation of plasma adiponectin concentrations was performed as needed to improve normality. (C) Age-specific prevalence of hypoadiponectinemia. Men (n=438), women (n=139).

Health and Welfare of Japan, and subjects who visited Osaka University Hospital for health check because of mild obesity [84 cases, 41 men (45±12 years), 43 women (58± 13 years)] were enrolled in the study. Informed consent was obtained from all subjects following the approval of the ethics committee of Osaka University. Among 661 subjects, 41 (6.2%), 49 (7.4%) and 34 (5.1%) were being treated with an anti-hypertensive, anti-hyperlipidemic or anti-diabetic regimen, respectively. Therefore, not all the subjects were clinically normal, but were almost representative of the general Japanese population. Diabetic subjects treated with insulin were not included in this study. We and others have reported that thiazolidinediones increase plasma adiponectin concentrations dramatically, so none of the subjects in our study group were receiving thiazolidinediones.

Anthropometry and Abdominal Fat Distribution

Anthropometric measurements (height, weight and waist circumference) were performed in a standing position. Body mass index (BMI) was calculated as weight divided by the square of height in meters. Waist circumference (WC) at the umbilical level was measured in the late exhalation phase while standing, as reported previously[23] Blood pressure was measured in the sitting position. A computed tomography (CT) scan was performed in all subjects in the routine supine position. The intra-abdominal visceral fat area (VFA) and subcutaneous fat area (SFA) were measured from CT cross-sectional scans at the level of the umbilicus, as reported previously[24]

Laboratory Measurements

Blood was withdrawn after an overnight fast and the plasma concentrations of adiponectin were measured by a sandwich enzyme-linked immunosorbent assay (ELISA) system (adiponectin ELISA kit, Otsuka Pharmaceutical Co), as reported previously[18] Plasma glucose and serum insulin concentrations at 0, 30, 60, and 120 min after 75-g oral glucose were determined by the glucose oxidase method and double-antibody radioimmunoassay, respectively. The sums of the glucose and insulin concentrations during the oral glucose tolerance test (OGTT) were calculated as Σglucose and Σinsulin. Serum total cholesterol and triglyceride concentrations were determined by enzymatic methods. High-density lipoprotein (HDL) cholesterol was also measured by an enzymatic method after heparin and calcium precipitation.

Table 1 Clinical Characteristics of the Study Subjects

	Men (n=479)	Women (n=182)
Age, years	53.1±9.5	55.7±9.5
BMI, kg/m²	24.0±3.5	24.2±4.1
WC, cm	86.3±8.9	82.3±11.6
Visceral fat area, cm²	105.7±52.8	77.4±45.1
Subcutaneous fat area, cm²	123.1±70.2	184.6±90.7
Adiponectin, μg/ml (min, max)	5.4 (0.8, 15.2)	8.2 (0.3, 20.9)
Category 1 <4.0, n (%)	109 (22.8)	16 (8.8)
Category 2 ≥4.0, < 5.5, n (%)	137 (28.6)	18 (9.9)
Category 3 ≥5.5, <7.0, n (%)	114 (23.8)	29 (15.9)
Category 4 ≥7.0, n (%)	119 (24.8)	119 (65.4)
Dyslipidemia, n (%)	255 (53.2)	60 (33.0)
Total cholesterol, mg/dl	198.8±32.5	209.2±31.0
Triglyceride, mg/dl	144.9±99.8	102.3±57.4
HDL cholesterol, mg/dl	50.8±14.5	64.0±17.3
Hypertension, n (%)	178 (37.2)	70 (38.7)
Systolic blood pressure, mmHg	123.8±17.2	121.6±21.5
Diastolic blood pressure, mmHg	73.8±12.3	70.9±14.0
High fasting glucose, n (%)	87 (18.2)	29 (15.9)
Fasting plasma glucose, mg/dl	99.9±22.3	97.1±21.8

BMI, body mass index; WC, waist circumference; HDL, high-density lipoprotein. Continuous variables, results are presented as mean±SD or median (minimum, maximum).

Table 2 Correlation Coefficients of the Relationships Between Plasma Adiponectin Concentration and Various Parameters of the Metabolic Syndrome

	Men (n=479)	Women (n=182)
Age	0.19****	0.14
BMI	−0.36****	−0.33****
WC	−0.32****	−0.33****
Visceral fat area	−0.29****	−0.24**
Subcutaneous fat area	−0.27****	−0.22**
Total cholesterol	−0.10*	0.02
Triglyceride	−0.36****	−0.29****
HDL cholesterol	0.26****	0.43****
Systolic blood pressure	−0.13**	−0.18*
Diastolic blood pressure	−0.20****	−0.17*
Fasting plasma glucose	−0.22****	−0.16*
Fasting plasma insulin	−0.18****	−0.29****
Σplasma glucose	−0.22****	−0.24**
Σplasma insulin	−0.14**	−0.30***

**p<0.05, **p<0.01, ***p<0.001, ****p<0.0001, Pearson's correlation coefficients.*
BMI, body mass index; WC, waist circumference; HDL, high-density lipoprotein; Σplasma glucose, sum of the glucose concentrations during the OGTT; Σplasma insulin, sum of the insulin concentrations during the OGTT.

Definition of the Metabolic Syndrome

There is not a current definition of the metabolic syndrome in Japan. In the present study, we tentatively defined it by modifying the criteria of the National Cholesterol Education Program's Adult Treatment Panel III report (NECP-ATP);[25] that is, the presence of at least 3 of the following abnormalities: (1) abdominal obesity: WC ≥85 cm in men or ≥90 cm in women according to the guidelines for diagnosis of 'Obesity Disease' in Japan;[26] (2) hypertriglyceridemia: a serum triglyceride concentration ≥150 mg/dl (1.69 mmol/L); (3) low HDL cholesterolemia: a serum HDL cholesterol concentration <40 mg/dl (1.04 mmol/L) according to the criteria of the Japan Atherosclerosis Society;[27] (4) hypertension: systolic blood pressure ≥130 mmHg, diastolic blood pressure ≥85 mmHg and/or having received antihypertensive medication; and (5) high fasting glucose: serum glucose concentration ≥110 mg/dl (6.1 mmol/L) and/or having received antidiabetic medication (oral agents).

Statistical Analysis

For continuous variables, results were expressed as mean±SD or median (minimum, maximum). Pearson's correlation coefficient was used to establish the association between plasma adiponectin concentrations and clinical parameters of the metabolic syndrome. Data that did not demonstrate Gaussian distribution were logarithmically transformed. The subjects were divided into 2 groups according to their adiponectin concentration (<4.0 μg/ml or >4.0 μg/ml). Category variables were represented by frequency counts, and comparisons between 2 groups were analyzed by the chi-square test. The interquartile cut-off points of plasma adiponectin concentration were 4.0, 5.5, and 7.0 μg/ml: category 1, <4.0 μg/ml; category 2, ≥4.0 μg/ml, <5.5 μg/ml; category 3, ≥5.5 μg/ml, <7.0 μg/ml; and category 4, ≥7.0 μg/ml as described previously?[28] The comparison of the mean number of components of the metabolic syndrome in each adiponectin quartile was analyzed by Kruskal-Wallis test with a Scheffe's test. All statistical analyses were performed with StatView-J 5.0 (SAS Inc).

Results

Prevalence of the Metabolic Syndrome and the Distribution of Plasma Adiponectin Concentration in the Japanese Population

Based on our criteria, 22.8% of men and 3.6% of women were diagnosed with the metabolic syndrome. In men, the prevalence increased from 13.3% among subjects aged 30–39 years to 27.7% among those aged 50–59 years, but decreased to 19.2% among men 60–69 years (Fig 1A). The prevalence of the metabolic syndrome in women was 4.2% and 5.7% for subjects aged 50–59 years and 60–69 years, respectively (Fig 1A). Therefore, the prevalence of the metabolic syndrome was highest in middle-aged men, and increased from the age of menopause in women.

Next, we determined the distribution of plasma adiponectin concentrations in this population and found that in both men and women the percentage of subjects was parametrically distributed against logarithmically transformed adiponectin concentrations (Fig 1B). The median concentration of plasma adiponectin was 6.1 μg/ml for the whole population sample. The distribution of the plasma adiponectin concentrations in men was lower than in women. The median concentrations of plasma adiponectin were 5.5 μg/ml in men and 8.7 μg/ml in women. We reported previously that subjects with a plasma adiponectin concentration less than 4.0 μg/ml had a 2-fold increase in the prevalence of CAD?[28] In the present study the prevalence of hypoadiponectinemia less than 4.0 μg/ml was 18.7% in men and 5.0% in women. The cut-off point of 4.0 μg/ml corresponded with median−1.4 median absolute deviation of the total subjects. The prevalence of hypoadiponectinemia in men and women was similar to that of the metabolic syndrome (Fig 1C).

Relationship Between Plasma Adiponectin Concentration and Each Component of the Metabolic Syndrome

We investigated the relationship between plasma adiponectin concentration and each component of the metabolic syndrome. The clinical characteristics and variables of the subjects are shown in Table 1. The correlation coefficient

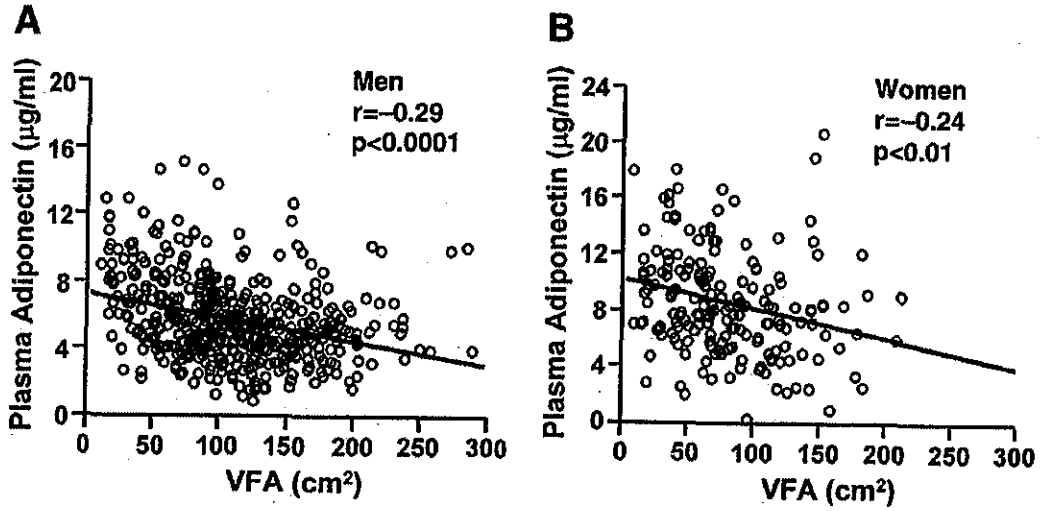

Fig 2. Correlation between visceral fat area (VFA) and plasma adiponectin concentration: men (n=479), women (n=182).

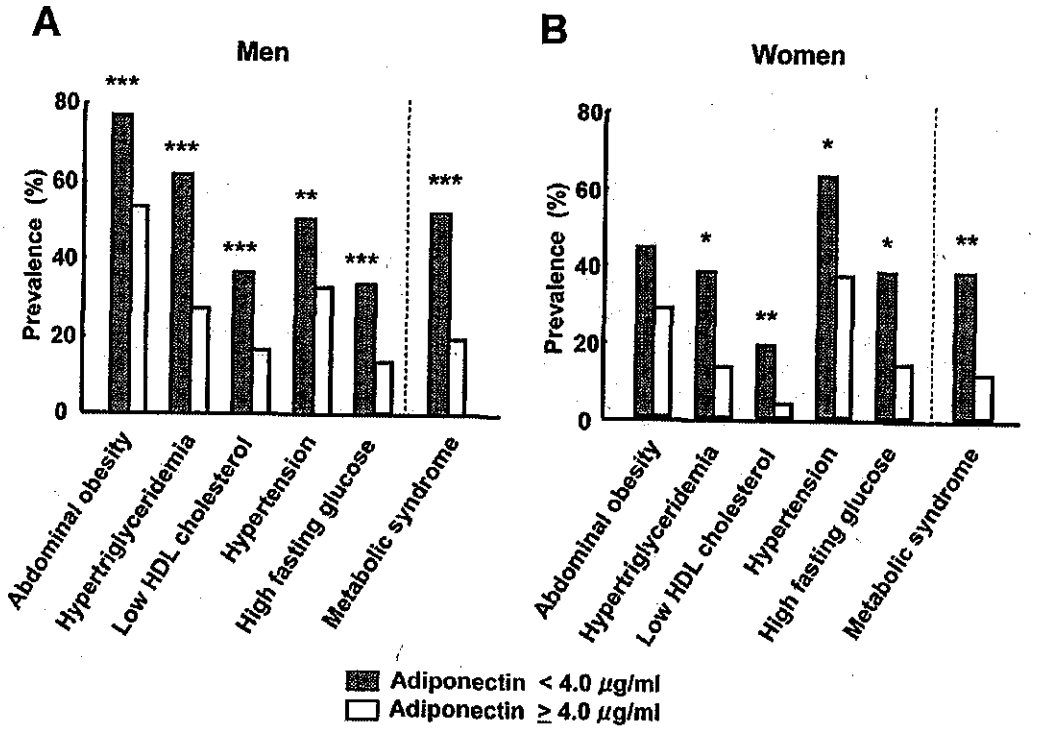

Fig 3. Prevalence of risk factors of the metabolic syndrome: men (n=479), women (n=182). *p<0.05, **p<0.01, ***p<0.001, Adiponectin <4.0μg/ml vs adiponectin ≥4.0μg/ml by chi-square test.

between plasma adiponectin and various parameters of the metabolic syndrome are shown in Table 2. With regard to the anthropometric parameters, plasma adiponectin concentration correlated negatively with BMI, WC, VFA, and SFA in both men and women. The correlation efficiency between plasma adiponectin concentration and VFA was r=–0.29 (p<0.0001) in men and r=–0.24 (p<0.01) in women (Fig 2). Among the parameters related to the metabolic syndrome, plasma adiponectin concentration correlated negatively with total cholesterol, triglyceride, systolic BP, diastolic BP, fasting plasma glucose, fasting plasma insulin, Σplasma glucose, and Σplasma insulin, and positively with HDL cholesterol in men. In women, plasma adiponectin levels correlated negatively with triglyceride, systolic BP, diastolic BP, fasting plasma glucose, fasting plasma insulin, Σplasma glucose, and Σplasma insulin, and positively with HDL cholesterol. No correlation was found between plasma adiponectin and total cholesterol in women. The presence of diabetes may affect the relationship between plasma adiponectin and Σplasma glucose or Σplasma insulin. However, similar results were obtained even when we excluded the diabetic subjects under medication (cor-